

Self-eXplainable AI for Medical Image Analysis: A Survey and New Outlooks

Junlin Hou, Sicen Liu, Yequan Bie, Hongmei Wang, Andong Tan, Luyang Luo, Hao Chen

Abstract—The increasing demand for transparent and reliable models, particularly in high-stakes decision-making areas such as medical image analysis, has led to the emergence of eXplainable Artificial Intelligence (XAI). Post-hoc XAI techniques, which aim to explain black-box models after training, have raised concerns about their fidelity to model predictions. In contrast, Self-eXplainable AI (S-XAI) offers a compelling alternative by incorporating explainability directly into the training process of deep learning models. This approach allows models to generate inherent explanations that are closely aligned with their internal decision-making processes, enhancing transparency and supporting the trustworthiness, robustness, and accountability of AI systems in real-world medical applications. To facilitate the development of S-XAI methods for medical image analysis, this survey presents a comprehensive review across various image modalities and clinical applications. It covers more than 200 papers from three key perspectives: 1) input explainability through the integration of explainable feature engineering and knowledge graph, 2) model explainability via attention-based learning, concept-based learning, and prototype-based learning, and 3) output explainability by providing textual and counterfactual explanations. This paper also outlines desired characteristics of explainability and evaluation methods for assessing explanation quality, while discussing major challenges and future research directions in developing S-XAI for medical image analysis.

Index Terms—Self-eXplainable Artificial Intelligence (S-XAI), Medical Image Analysis, Input Explainability, Model Explainability, Output Explainability, S-XAI Evaluation

I. INTRODUCTION

Artificial intelligence (AI), particularly deep learning, has driven significant advancements in medical image analysis, including applications in disease diagnosis, lesion segmentation, medical report generation (MRG), and visual question

This work was supported by the Hong Kong Innovation and Technology Fund (Project No. MHP/002/22), HKUST (Project No. FS111) and Research Grants Council of the Hong Kong (No. R6003-22 and T45-401/22-N).

J. Hou, Y. Bie, H. Wang, and A. Tan are with the Department of Computer Science and Engineering, Hong Kong University of Science and Technology, Hong Kong, China (email: csejlhou@ust.hk)

S. Liu is with the Department of Engineering, Shenzhen MSU-BIT University, Shenzhen, China (email: liusicen@smbu.edu.cn)

L. Luo is with the Department of Biomedical Informatics, Harvard University, Cambridge, USA (email: luyang.luo@hms.harvard.edu)

H. Chen is with the Department of Computer Science and Engineering, Department of Chemical and Biological Engineering and Division of Life Science, Hong Kong University of Science and Technology, Hong Kong, China; HKUST Shenzhen-Hong Kong Collaborative Innovation Research Institute, Futian, Shenzhen, China. (email: jhc@cse.ust.hk)

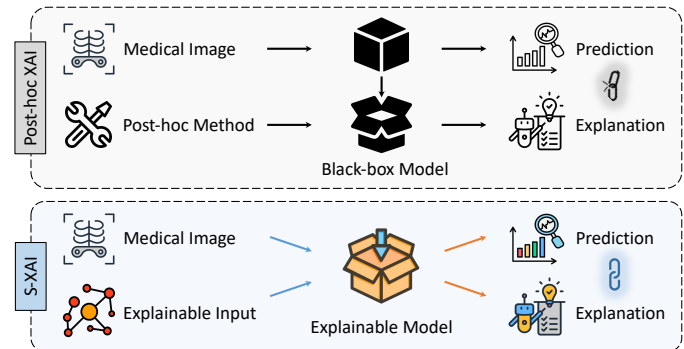


Fig. 1. Illustration of post-hoc XAI versus Self-eXplainable AI (S-XAI).

answering (VQA). Deep neural networks (DNNs) automatically learn features from input data and produce optimal outputs. However, the inherent complexity nature of DNNs hinder our understanding of the decision-making processes behind these models. Consequently, DNNs are often considered as black-box models, which has raised concerns about their transparency, interpretability, and accountability for their successful deployment in real-world clinical applications [1].

To tackle the challenge of developing more trustworthy AI systems, research efforts are increasingly focusing on various eXplainable AI (XAI) methods, enhancing transparency [2], fairness [3], and robustness [4]. However, most XAI methods aim to generate explanations for the outputs of black-box AI models after they have been trained, a category known as post-hoc XAI, as illustrated in Fig. 1 top. These methods utilize additional explanation models or algorithms to provide insights into the decision-making process of the primary AI model. In the field of medical image analysis, commonly used post-hoc XAI techniques include feature attribution methods, such as gradient-based approaches (e.g., LRP [5], CAM [6]) and perturbation-based approaches (e.g., LIME [7], Kernel SHAP [8]). Additionally, some methods explored concept attributions, learning human-defined concepts from the internal activations of DNNs (e.g., TCAV [9], CAR [10]). Post-hoc XAI techniques are often model-agnostic, indicating that they can be flexibly applied to a variety of already-trained black-box AI models.

Since post-hoc explanations are generated separately from the primary AI model, several valid concerns have been raised: 1) these explanations may not always be faithful to the actual decision-making process of black-box models [11], [12]; 2) they may lack sufficient detail to fully elucidate the model's functioning [13]. These limitations of post-hoc XAI approaches are particularly problematic in high-stakes

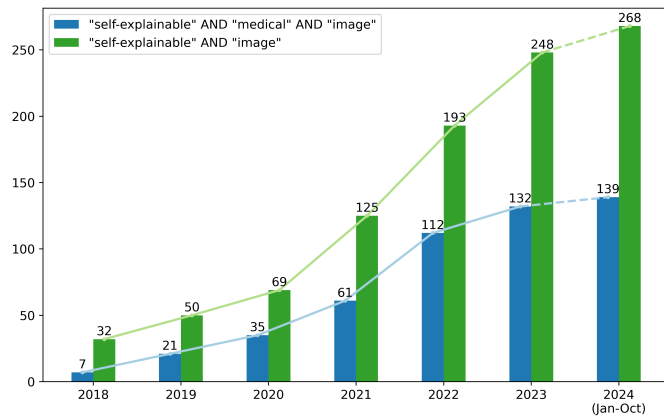


Fig. 2. The upward trend of the total number of S-XAI research papers from 2018 to 2024 (Jan-Sept), where medical articles account for half.

domains like medical image analysis, where clinicians require a deep and trustworthy understanding of how an AI model arrives at its predictions. The issues about the faithfulness and sufficiency of post-hoc explanations highlight the importance of exploring self-explainable AI models as a potentially more reliable and transparent alternative.

Self-explainable AI (S-XAI) is a category of XAI methods designed to be interpretable by nature, as illustrated in Fig. 1 bottom. These methods incorporate explainability as an integral part of the model during the training process, rather than generating explanations after the model has been trained. Conventional inherently interpretable methods include various white-box machine learning models, such as decision trees [14], generalized additive models [15], and rule-based systems [16]. In this survey, we focus primarily on DNNs and extend the characteristics of self-explainability across the entire pipeline, from model input to architecture to output, enabling direct inspection and understanding of the reasoning behind the model's predictions without reliance on external explanation methods. In contrast to post-hoc XAI approaches, S-XAI methods aim to provide explanations that are inherent, transparent, and faithful, aligning directly with the model's internal decision-making mechanisms. Such explanations are essential for the effective adoption and clinical integration of AI-powered decision support systems. Furthermore, S-XAI facilitates collaborative decision-making between clinicians and AI systems, fostering better-informed and more accountable medical diagnoses and interventions.

This paper presents the first systematic review of S-XAI for medical image analysis, covering methodology, medical applications, and evaluation metrics, while also offering an in-depth discussion on challenges and future directions. Although there is a wealth of literature on medical XAI surveys [2], [17]–[22] that deliver valuable insights, none have focused specifically on a comprehensive review of S-XAI methods applied to medical image analysis. We analyze more than 200 papers published from 2018 to October 2024, sourced from the proceedings of NeurIPS, ICLR, ICML, AAAI, CVPR, ICCV, ECCV, and MICCAI as well as top-tier journals in the field, including Nature Medicine, Transactions on Pattern Analysis and Machine Intelligence, Transactions on Medical Imaging, Medical Image Analysis, or those cited in related

works. The statistics of research articles using keywords *self-explainable*, *medical*, *image* on Google Scholar are presented in Fig. 2, which reveal two key observations: 1) there has been a significant and consistent increase in research papers focused on self-explainable AI over the years, indicating growing interest and emphasis within the research community; 2) nearly half of the total research papers (green bars) are dedicated to applying S-XAI techniques in medical imaging (blue bars), highlighting the vital importance of S-XAI in the medical field.

To summarize, this survey presents insights into S-XAI for medical image analysis, with our contributions outlined below:

- 1) **Novel scope of XAI survey:** As an emerging XAI method that actively offers explainability from the model itself, S-XAI is attracting growing attention from the research community. This work serves as the first comprehensive survey on this topic.
- 2) **Systematic review of methods:** We introduce a novel taxonomy of relevant papers and review them based on input explainability, model explainability, and output explainability. This offers insights into potential technical innovations for S-XAI methods.
- 3) **Thorough overview of applications:** We overview various downstream applications across different anatomical locations and modalities in current S-XAI research. This illustrates the ongoing development of S-XAI technologies in medical image analysis, serving as a reference for future applications in diverse contexts.
- 4) **Comprehensive survey of evaluations:** We analyze a range of desired characteristics and evaluation methods to assess the quality of explainability. This provides guidelines for developing clinically explainable AI systems that are trustworthy and meaningful for end-users.
- 5) **In-depth discussion of challenges and future work:** We discuss the key challenges and look forward to the promising future directions. This underscores existing shortcomings and identifies new outlooks for researchers to drive further advancements.

II. S-XAI IN MEDICAL IMAGE ANALYSIS

Transparency and trustworthiness are essential for deep learning models deployed in real-world applications of medical image analysis. To address this need, the research community has explored various XAI methods and proposed several XAI taxonomy. According to existing literature [17], [19], [23], XAI methods can be categorized by the following criteria.

1) **Intrinsic versus Post-hoc:** This criteria differentiates whether interpretability is inherent to the model's architecture (intrinsic) or achieved after the model training (post-hoc).

2) **Model-specific versus Model-agnostic:** Model-specific methods are restricted to particular model classes, whereas model-agnostic methods can be applied to explain any model;

3) **Local versus Global:** The scope of an explanation distinguishes between those for an individual prediction (local) or those for the entire model behavior (global).

4) **Explanation modality:** The common types of explanation include visual explanation, textual explanation, concept explanation, sample explanation, etc.

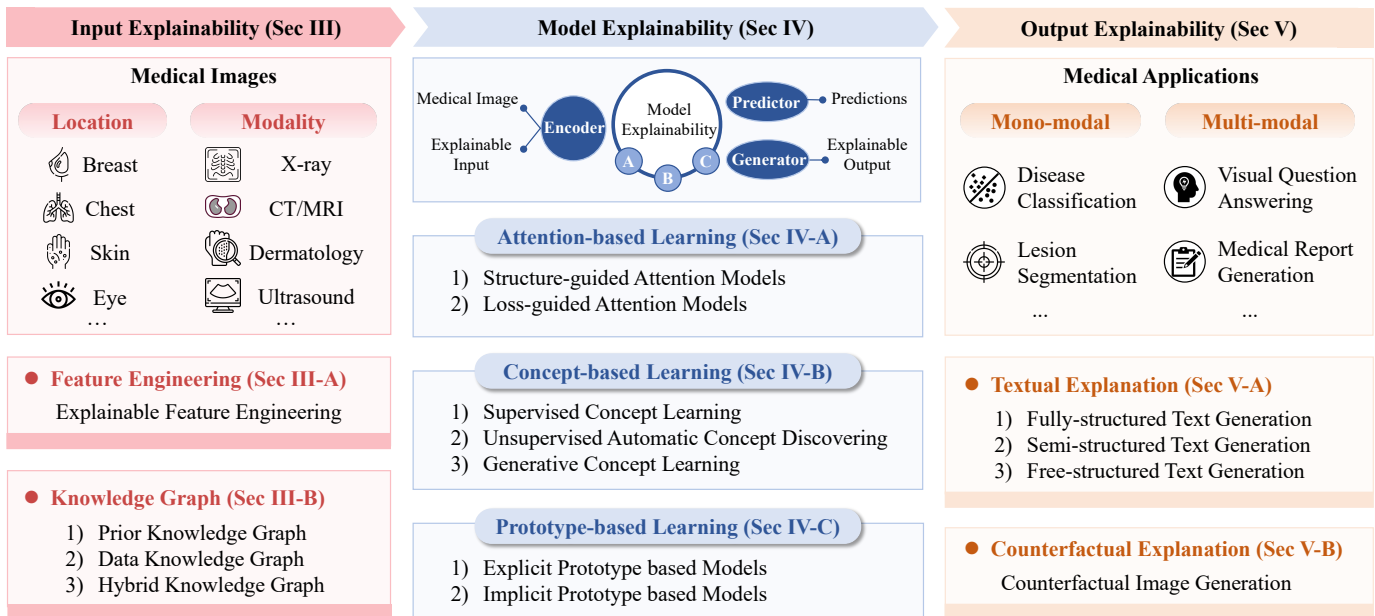


Fig. 3. Overview of Self-explainable AI (S-XAI) frameworks including input explainability, model explainability, and output explainability.

This survey concentrates on S-XAI methods for medical image analysis that allow models to inherently explain their own decision-making. As depicted in Fig. 3, we introduce a new taxonomy of S-XAI based on the three key components of DNNs.

1) Input explainability (Sec. III): Input explainability focuses on integrating additional explainable inputs with deep features of medical images obtained from various anatomical locations and modalities to produce final predictions. By incorporating external knowledge and context-specific information, the accuracy and reliability of these predictions can be significantly improved.

2) Model explainability (Sec. IV): Model explainability aims to design inherently interpretable model architectures of DNNs. Instead of explaining a black-box model, transforming the model into an interpretable format enhances understanding of how it processes information.

3) Output explainability (Sec. V): Output explainability refers to the model's ability to generate not just predictions for various medical image tasks but also accompanying explanations through an explanation generator. This capability aids in understanding the rationale behind the model's predictions, facilitating informed medical decision-making.

The following sections summarize and categorize the most relevant works on S-XAI methods applied to medical image analysis. Comprehensive lists of the reviewed S-XAI methods are provided, detailing the employed S-XAI techniques, publication year, anatomical location, image modality, medical application, and the datasets used.

III. INPUT EXPLAINABILITY

In this section, we will explore input explainability by integrating external domain knowledge, focusing on two key approaches, i.e., a) explainable feature engineering (Sec. III-A) and b) knowledge graph (Sec. III-B). As shown in Fig. 4, these explainable inputs will interact with the deep features of image inputs and be combined to support final predictions.

A. Explainable Feature Engineering

Feature engineering aims to transform raw images into a more useful set of human-interpretable features [24], which is essential for traditional machine learning. However, deep learning models automatically extract features from raw images, simplifying the handcraft process but often sacrificing interpretability. To enhance input explainability, it is beneficial to combine explainable feature engineering with deep learning, as shown in Fig. 4A. This integration enhances models' interpretability by injecting domain knowledge into models and ensuring that the learned features are relevant and meaningful for clinical applications.

A common strategy is to combine both deep and handcrafted features from an input image to make final predictions [25], [26]. For example, Kapse *et al.* [25] introduce a self-interpretable multiple instance learning framework that simultaneously learns from deep image features and handcrafted morphometric and spatial descriptors. Local and global interpretability are demonstrated through quantitative and qualitative benchmarking. Another line of approach involves incorporating interpretable clinical variables as additional inputs alongside images, often utilizing multimodal learning techniques [27], [28]. For instance, Xiang *et al.* [27] introduce OvcaFinder, an interpretable model that combines deep learning predictions from ultrasound images with Ovarian-Adnexal Reporting and Data System scores provided by radiologists, as well as routine clinical variables for diagnosing ovarian cancer. This approach enhances diagnostic accuracy and explains the impact of key features and regions on the prediction outcomes.

Discussion: Although explainable feature engineering can be time-consuming, it brings valuable prior knowledge and enhances the interpretability of deep learning models concerning input features. Despite the increasing research in this area, most studies prioritize accuracy improvements, with limited analysis given to the explainability. Additionally, effective information fusion and interaction poses a key challenge.

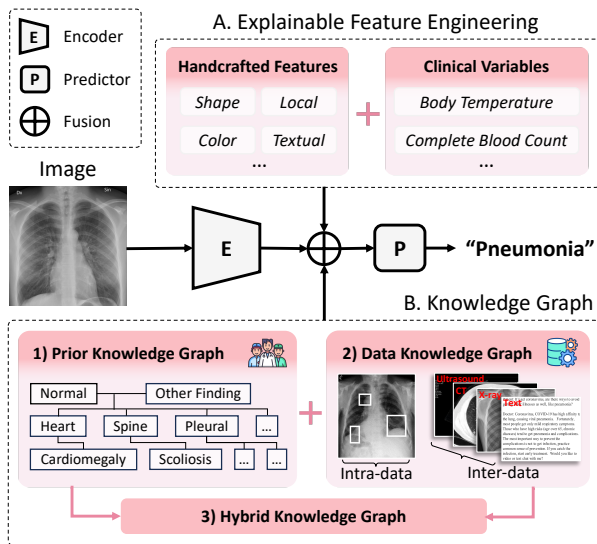


Fig. 4. Input explainability that incorporates explainable feature engineering and knowledge graphs as additional inputs.

B. Knowledge Graph

A knowledge graph (KG) is a structured representation of factual knowledge that captures relationships between entities in the real world [29]. Recently, there has been increasing interest in integrating structured domain knowledge into downstream applications [30]–[32], with the recognition that leveraging domain knowledge can greatly improve the performance and self-explainability of deep learning models. Regarding medical image analysis, the types of KG can be broadly categorized into three categories: 1) prior KG, which serves as a foundational resource that gathers existing domain expertise; 2) data KG, which is derived from the analysis of large-scale medical image datasets; and 3) hybrid KG, which combines prior KG and data KG, as illustrated in Fig. 4B.

1) *Prior knowledge graph*: In the medical domain, prior KG captures and organizes factual information about medical concepts and their relationships, which can be constructed from multiple sources, such as medical literature, medical ontologies, clinical guidelines, and expert opinions. It serves as a comprehensive repository of medical knowledge, encompassing details about diseases, symptoms, treatments, medications, anatomical structures, and provides a vital foundation for medical decision-making, clinical research, and healthcare analytics [33]–[35]. By harnessing the medical prior knowledge encoded in the graph, AI models introduce specialized domain information during the input phase and leverage this prior knowledge to enhance model’s self-explainability, gain valuable insights, and improve the performance of AI model in clinical task such as Med-VQA [36], [37] and medical report generation [38]–[41]. For example, Zhang *et al.* [38] construct prior graphs from clinical studies to support radiology report generation. Huang *et al.* [40] develop symptom graphs based on a professional perspective of medical images, injecting the model with the ability to understand these images, thereby generating reliable medical reports. Liu *et al.* [41] extract a set of 52.6K triplets containing medical knowledge from OwnThink (<https://www.ownthink.com>) and use this external

information to create SLAKE, a knowledge-enhanced bilingual dataset for training and testing Med-VQA systems. Prior KGs enhance S-XAI models by integrating medical facts. However, the creation of these KGs largely depends on specialized expertise, which makes the process labor-intensive and time-consuming. Furthermore, they often lack the adaptability required for analyzing dynamic clinical datasets.

2) *Data knowledge graph*: Unlike prior KG, which relies on expert insights, data KG is built directly from the dataset itself, giving them the potential to discover previously unknown relationships and correlations [42]–[44]. There are two main types of data KG for enhancing the explainability of AI models. 1) Intra-data KG is a local relation graph within a data sample [45]–[49]. For instance, Chen *et al.* [45] propose label co-occurrence learning to explore the relationship between pathologies in multi-label chest X-ray image classification. Huang *et al.* [48] construct the medical KG based on the types of diseases and questions from a Med-VQA dataset and propose a medical knowledge-based VQA network. 2) Inter-data KG captures relationships between different data samples [50], [51]. For example, Zheng *et al.* [50] utilize six meta-paths to connect four types of data (i.e., X-ray, CT, ultrasound, and text descriptions of diagnosis) and create a multi-modal KG for COVID-19 diagnosis. Furthermore, Zhao *et al.* [52] and Qi *et al.* [53] leverage both intra-data and inter-data graph into a unified framework for disease diagnosis and localization in X-rays. Constructing a data KG involves leveraging the inherent characteristics of the dataset itself to assist S-XAI models. However, these methods would harbor inherent biases that can vary significantly across different datasets.

3) *Hybrid knowledge graph*: Hybrid KG integrates prior KG and data KG, which not only provides a foundation of established medical facts, but also allows for the integration of new information and the refinement of existing knowledge. Consequently, hybrid KG combines strengths of both prior KG and data KG, offering a more comprehensive and adaptable knowledge representation for S-XAI models in the medical field [54]–[60]. For instance, Zhou *et al.* [54] combine intra- and inter-contrastive attentions to learn abnormal attended visual features of X-rays and then leverage a chest radiology prior KG to enhance the thoracic disease diagnosis models. To enable dynamic graph construction, Li *et al.* [57] initially utilize a foundational structure from prior KG and then add nodes or modify their relationships based on the specific knowledge relevant to each X-ray image. Moreover, Hu *et al.* [60] use large language models to extract labels and build a large-scale medical VQA dataset, and then leverage graph neural networks to learn logical reasoning paths.

Discussion: The utilization of medical KGs for S-XAI poses both challenges and promising opportunities. First, integrating diverse prior medical knowledge into a graph format is labor-intensive and costly, requiring constant updates and refinements to incorporate the latest knowledge. Another challenge lies in the heterogeneity of medical data. The expanding variety of data modalities would complicate the effective integration within KGs. Developing robust AI algorithms to extract meaningful features from medical data and align them with medical KGs remains an ongoing research endeavor.

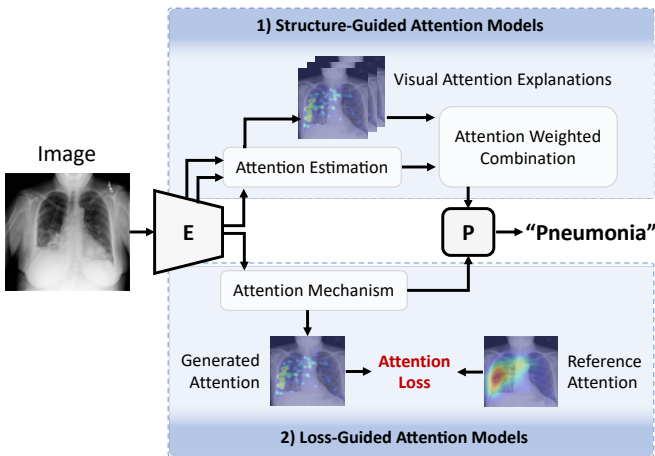


Fig. 5. Attention-based learning, including 1) structure-guided and 2) loss-guided attention models. X-ray images borrowed from [62].

IV. MODEL EXPLAINABILITY

In this section, we present model explainability by designing interpretable model architectures, such as attention-based learning (Sec. IV-A), concept-based learning (Sec. IV-B), and prototype-based learning (Sec. IV-C).

A. Attention-based Learning

Attention-based learning aims to capture specific image regions that are relevant to specific model task while suppressing irrelevant regions based on attention maps [61]. Therefore, attention-based models can provide visual explanations that interpret model decision-making [2], [19]. We categorize attention-based S-XAI models into 1) structure-guided attention models and 2) loss-guided attention models. As illustrated in Fig. 5, the former estimates attention scores through structural design, whereas the latter constrains attention maps using loss functions.

1) *Structure-guided attention models*: As shown in the top branch of Fig. 5, structure-guided attention models are characterized by the attention estimator whose outputs directly influence model’s predictions. The estimator structure combine the features from different encoder-layer features to calculate feature attention scores as the generated attention map to effectively explain the model’s predictions [63]–[65]. For example, Jetley *et al.* [63] first introduce attention-based learning for XAI by proposing an attention estimator to calculate feature compatibility scores and weigh feature maps, which are then used directly as input for a linear classifier. Numerous studies have incorporated multiple attention mechanisms for medical image classification and segmentation tasks [65]–[70]. For example, Schempler *et al.* [67] extend the attention estimator by extracting local information from coarse features for attention gates, facilitating more fine-grained visual interpretation for lesion segmentation and ultrasound diagnosis. Similarly, Gu *et al.* [69] develop a comprehensive attention module with spatial, channel, and scale attention. The segmentation results on skin lesions and fetal organs demonstrate improved performance and better interpretability of target area positioning and scale. Beyond 2D data, how to use attention to explain more complex 3D medical image analysis is more challenging. Lozupone *et al.* [70] present an

attention module that fuses attention weights from sagittal, coronal, and axial slices to diagnose Alzheimer’s disease on 3D MRI brain scans, in which 3D attention maps can be visualized to explain the model’s decision-making process. For fast MRI reconstruction, Huang *et al.* [71] propose a shifted windows deformable attention mechanism which uses reference points to impose spatial constraints on attention and combines the attention outputs from different windows to produce reconstruction results. Although structure-guided attention models can provide explanations for predictions, they are still difficult to align with clear human-understandable decision-making basis.

2) *Loss-guided attention models*: As shown in the bottom branch of Fig. 5, loss-guided attention models use interpretable labels (i.e., reference attention maps) to constrain generated attention maps from attention mechanism by loss functions. Using ground-truth masks of regions of interest (RoIs) to guide the generation of attention maps is a widely adopted approach in medical image classification [62], [72]–[75]. For instance, Yang *et al.* [72] directly optimize the attention maps by a Dice loss, which encourages the model to focus on target areas that are highly relevant to the classification of breast cancer microscopy images. To alleviate the challenge of obtaining pixel-level annotations, Yin *et al.* [75] pre-train a histological feature extractor to identify significant clinically relevant feature masks, which are then used to guide and regularize attention maps. By considering the varying contributions of histological features for classification, the model can selectively focus on different features based on the distribution of nuclei in each instance. In medical image segmentation, labels corresponding to edges and shapes of specific regions are often reused to guide attention in learning semantic information [76]–[78]. Sun *et al.* [76] combine spatial attention with the attention estimator in U-Net decoders, enabling the model to interpret learned features at each resolution. They also introduce a gated shape stream alongside the texture stream, where the shape attention maps are aligned with actual edges by a binary cross-entropy loss, enhancing cardiac MRI segmentation.

Compared with lesion masks, eye tracking data provides a more accurate depiction of expert focus, as it captures the way doctors visually process information during diagnosis. Bhattacharya *et al.* [62] leverage the captured doctors’ attention to guide model training. They employ a teacher-student network to replicate the visual cognitive behavior of doctors when diagnosing diseases on chest radiographs. The teacher model is trained based on the visual search patterns of radiologists, and the student model utilizes an attention loss to predict attention from the teacher network using eye tracking data.

Discussion: Attention-based S-XAI methods offer effective visual explanations. Structure-guided attention models use attention-weighted outputs as inputs for predictors, reflecting decision-making but often lacking clear semantic information. In contrast, loss-guided attention models provide explicit semantic details in their explanations, though their attention outputs do not directly influence model decisions. Overall, while these methods improve transparency and insights into decision-making, the understandability of attention maps and their relevance still require further investigation.

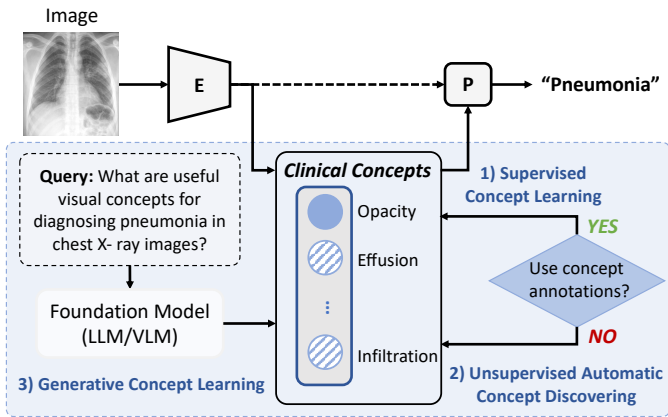


Fig. 6. Concept-based learning, including 1) supervised concept learning, 2) unsupervised automatic concept discovering, and 3) generative concept learning.

B. Concept-based Learning

Concept-based S-XAI methods provide explanations in terms of high-level, human-interpretable attributes rather than low-level, non-interpretable features, enabling users to gain deeper insights into the underlying reasoning with easily understandable concepts [9], [79]. It also helps in identifying model biases and allows for adjustments to enhance performance and trustworthiness. Most concept-based S-XAI methods focus on making decisions based on a set of concepts while also detailing the contribution of each concept to the final prediction [80]–[83]. We propose to categorize concept-based S-XAI methods into three types: 1) supervised concept learning, 2) unsupervised automatic concept discovering, and 3) generative concept learning, as shown in Fig. 6.

The term *Concept* has been defined in different ways, which commonly represents high-level attributes [9], [79], [84]. In this paper, we suggest adopting a simple and clear categorization: *Textual Concepts* and *Visual Concepts*. *Textual Concepts* refer to textual descriptions of attributes associated with the classes. For example, in Fig. 6, the textual concepts for the classes (i.e., “pneumonia” and “normal”) include terms like *Opacity*, *Effusion*, *Infiltration*, etc. *Visual Concepts*, on the other hand, consist of semantically meaningful features within the image that may not be explicitly described in natural language. For example, Alvarez Melis *et al.* [4] consider the intermediate image representations in a space of interpretable atoms with low dimension as the concepts of a given image.

1) *Supervised concept learning*: Supervised concept learning methods train deep learning models using annotations of textual concepts, particularly by supervising an intermediate layer to represent these concepts. A notable example is Concept Bottleneck Model (CBM) [80], which first maps latent image features to a concept bottleneck layer, where the number of neurons corresponds to the number of human-defined concepts, and then predicts final results based on the concept scores from this layer. Learning concept representations supervised by concept labels enables CBMs to directly show each concept’s contribution to the final prediction using the neuron values of the last layer. Additionally, CBMs allow model editing. When domain experts find certain predicted concept importance unreasonable, they can adjust the model’s

predictions by modifying the weights of the concept bottleneck layer (i.e., test-time intervention). The CBM architecture has inspired many researchers to develop self-explainable methods, resulting in a series of CBM-like models [85]–[87].

The self-explainable nature of concept-based learning models has led to its application in medical imaging to satisfy the trustworthiness requirements of healthcare [88]–[98]. Chauhan *et al.* [88] propose Interactive CBMs, which can request labels for certain concepts from a human collaborator. This method exhibits good interpretability on chest and knee X-ray datasets. Kim *et al.* [95] present a medical concept retriever, which connects medical images with text and densely scores images on concept presence. This work uses a CBM architecture to develop an inherently interpretable model and conducts data auditing and model interpretation. Different from CBMs, Concept Whitening [99], [100] aims to whiten the latent space of neural networks and aligns the axes of the latent space with known concepts of interest. Zhao *et al.* [101] introduce a hybrid neuro-probabilistic reasoning algorithm for verifiable concept-based medical image diagnosis, which combines clinical concepts with a Bayesian network. However, a significant challenge in supervised concept learning is the scarcity of concept annotations, which require labor-intensive efforts from human experts. Therefore, some researchers prefer unsupervised automatic concept discovering, as it eliminates the need for extra annotations.

2) *Unsupervised automatic concept discovering*: These models modify their internal representations to identify visual concepts within image features, without relying on explicit annotations. The discovered concepts may not be directly associated with human-specified textual concepts, but can also be visualized and detailed their contributions to final predictions. Self-Explaining Neural Networks (SENN) [4] first utilize a concept encoder to extract clusters of image representations corresponding to different visual concepts, and adopt a relevance parametrizer to calculate the relevance scores of concepts. The final prediction is determined by the combination of discovered concepts and the corresponding relevance scores. Inspired by SENN, Sarkar *et al.* [102] utilize both a concept encoder and a concept decoder, which map images into concept space and use the concepts to reconstruct the original images, respectively. Since medical concept annotations are costly and require experts’ efforts, unsupervised automatic concept discovering is usually adopted to offer concept-based explanations in medical image analysis without expert-annotated labels. For example, Fang *et al.* [103] address the practical issue of classifying infections by proposing a visual concept mining method to explain fine-grained infectious keratitis images. They first use a saliency map based potential concept generator to discover visual concepts, and then propose a visual concept-enhanced framework that combines both image-level representations and the discovered concept features for classification. Although unsupervised automatic concept discovering can offer concept-based explanations, these explanations are abstract and usually cannot be directly described in natural language. To alleviate this issue while also addressing the lack of concept annotations, generative concept learning has become a promising research direction.

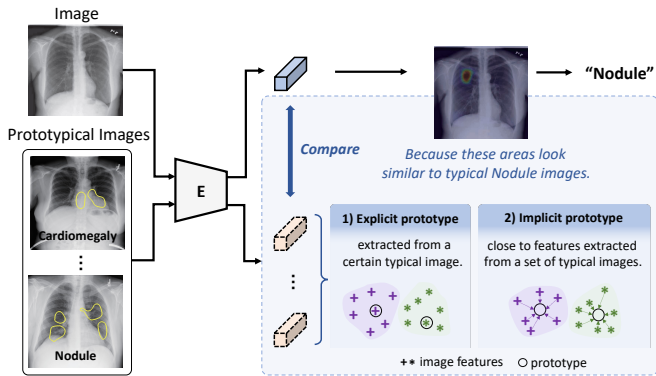


Fig. 7. Prototype-based learning, including 1) explicit prototype and 2) implicit prototype. X-ray images borrowed from [112].

3) *Generative concept learning*: Leveraging foundation models, such as Large Language Models (LLMs) and Vision-Language Models (VLMs), can assist in generating and labeling textual concepts. A notable generative concept learning method, namely Language Guided Bottlenecks (LaBo) [104], employs an LLM (GPT-3 [105]) to generate textual concepts for each image category, which are filtered to form the concept bottleneck layer. LaBo then uses a pre-trained VLM (CLIP [106]) to calculate the similarity between input images and the generated concepts to obtain concept scores. The final prediction is based on the multiplication of a weight matrix and these concept scores. Label-free CBM [107] employs a similar pipeline, but trains an independent network that includes a concept bottleneck layer. In the medical domain, Kim *et al.* [108] enhance LaBo by incorporating a more fine-grained concept filtering mechanism and conduct explainability analysis on dermoscopic images, achieving performance improvements compared to the baseline. Similarly, some research [109], [110] employ ChatGPT and CLIP for explainable disease diagnosis. Bie *et al.* [111] propose an explainable prompt learning framework that leverages medical knowledge by aligning the semantics of images and clinical concept-driven prompts at multiple granularities, where category-wise clinical concepts are obtained by eliciting knowledge from LLMs.

Discussion: Concept-based learning hold significant importance in medical research and applications, particularly in advancing evidence-based medicine. The lack of fine-grained concept annotations and the performance-explainability trade-off are the limitations of concept-based methods. As there are more and more medical foundation models being developed, incorporating knowledge from these models and medical experts to efficiently annotate concept labels for datasets will be a promising and meaningful direction. Besides the most popular classification task, other medical applications of concept-based approaches should be further explored.

C. Prototype-based Learning

Prototype-based S-XAI models aims to provide a decision-making process where a model reasons through comparisons with a set of interpretable example prototypes. This reasoning aligns with human recognition patterns, as humans often identify objects by comparing them to example components [113]. These models first extract features from a given image and

then compare the feature maps with the prototypes to calculate similarities. This process is considered interpretable because the decision making can be clearly attributed to the contribution of each interpretable prototype (e.g., by the similarity scores). According to how the prototypes are obtained, we define and categorize them to two types: 1) explicit prototype and 2) implicit prototype, as presented in Fig. 7. Explicit prototypes are specific high-dimensional feature representations extracted from certain training images, whereas implicit prototypes are latent high-dimensional representations that are close to a set of typical images' representations. All existing prototype-based S-XAI models do not require supervision at the prototype level and aim to automatically find meaningful prototypes to facilitate interpretable decision making.

1) *Explicit prototype based models*: The first model of this type is ProtopNet [114], which introduces a three-stage training scheme: 1) Freeze the final layer, and only train the feature extractor. 2) Replace the learned representations in the prototype layer with the nearest feature patch from the training set. 3) Remain the feature extractor fixed and fine-tune the parameters of the final layer. Later works closely follow this training scheme while addressing different limitations of this initial framework [115]–[122]. Adopting prototype-based S-XAI models in the medical domain presents additional challenges. Unlike natural images where the representative prototype occupies an area with a relatively stable size, medical image features such as disease regions in chest X-ray images can vary significantly in size. To address this, XProtoNet [112] proposes to predict an occurrence map and summing the similarity scores within those areas, rather than relying solely on the maximum similarity score as done in ProtopNet. Similarly, [123] introduces prototypes with square and rectangular spatial dimensions for COVID-19 detection in chest X-rays. In evaluations of ProtopNet, Mohammadjafari *et al.* [124] observe a performance drop for Alzheimer's disease detection using MRI, whereas Carlon *et al.* [125] report a high-level of interpretability satisfaction from radiologists in breast mass classification using mammograms. In mammogram based breast cancer diagnosis, Wang *et al.* [126] propose to leverage knowledge distillation to improve model performance. To overcome the confounding issue in mammogram based mass lesion classification, Barnett *et al.* [127] employ a multi-stage framework that identifies the mass margin features for malignancy prediction, skipping image patches that have already been used in previous prototypes during the prototype projection step to improve prototype diversity. In brain tumor classification, MProtoNet [128] introduces a new attention module with soft masking and online-CAM loss applied in 3D multi-parametric MRI. To predict the brain age based on MR and ultrasound images, Hesse *et al.* [129] utilize the weighted mean of prototype labels. Additionally, INSightR-Net [130] formulates the diabetic retinopathy grading as a regression task and apply the prototype based framework, while ProtoAL [131] explores an active learning setting for prototype-based models in diabetic retinopathy.

Although these models offer interpretability in a one-to-one mapping to the input image, they can also make it difficult for users to identify which specific property is important in the

corresponding image patch (e.g., is it the color or texture that matters in this prototypical area?). This issue can be partially mitigated using implicit prototype based models.

2) *Implicit prototype based models*: This type of model follows a similar training scheme as the models based on explicit prototypes, with the major difference in avoiding the prototype replacement step, or only projecting the prototype to the training images' feature patches for visualizations. This scheme is simpler than one that includes prototype replacement step and has different interpretability benefits. Li *et al.* [132] propose the earliest work using latent prototypes, which leverages a decoder to visualize the meanings of the learned prototypes. Protoeval [133] designs a set of loss functions to encourage the learned latent prototypes to be more stable and consistent across different images. Recently, to address the concern that prototype-based models often underperform their black box counterparts, Tan *et al.* [134] develop an automatic prototype discovery and refinement strategy to decompose the parameters of the trained classification head and thus guarantees the performance. Although a series of implicit prototype based models [135]–[137] are demonstrated effectiveness on natural images, their developments and applications on medical image analysis need to be further explored.

Discussion: In terms of performance, implicit prototype based models generally outperform explicit ones, probably due to the greater flexibility in prototype learning. Regarding interpretability, both types of models offer unique advantages. Explicit prototypes can be intuitively explained through one-to-one mappings to the input image, while implicit prototypes can be explained using a diverse set of images with similar activations. However, current prototype-based S-XAI models in medical image analysis primarily use explicit prototypes, making the exploration of implicit prototypes in this domain a promising area for future research.

V. OUTPUT EXPLAINABILITY

This section discusses output explainability by generating explanations alongside model predictions, including textual (Sec. V-A) and counterfactual (Sec. V-B) explanations.

A. Textual Explanation

S-XAI models that provide textual explanations generate human-readable descriptions to accompany their predictions as part of outputs, similar to image captioning. These methods use natural language to clarify model decisions and typically require textual descriptions for supervision. Some studies explore the integration of textual explanations with visual ones. We categorize these methods into three types based on the structure of textual explanations: 1) fully-structured, 2) semi-structured, and 3) free-structured text, as shown in Fig. 8(a).

1) *Fully-structured text generation*: To address the challenges posed by complex unstructured medical reports, early efforts transformed target texts into fully structured formats, such as descriptive tags [139], attributes [140], [141] with fixed templates, rather than natural language. For example, Medical Subject Headings (MeSH) [142] can be utilized to describe image content instead of unstructured reports. Therefore, both Shin *et al.* [143] and Gasimova *et al.* [144] employ CNN-RNN

frameworks to identify diseases and generate corresponding MeSH sequences, detailing location, severity, and affected organs in chest X-ray images. However, complete descriptions in natural language are more human-understandable than a set of simple tags, leading several studies to focus on generating reports in a semi-structured format.

2) *Semi-structured text generation*: Generating semi-structured text involves a partially structured format with predefined topics and constraints. For instance, pathology report generation methods [145]–[147] produce reports that focus on describing certain types of cell attributes along with a concluding statement. Additionally, Wang *et al.* [148] introduce a hierarchical framework for medical image explanation, which first predicts semantically related topics and then incorporates these topics as constraints for the language generation model. More recently, some studies have focused on generating individual sentences based on anatomical regions [149]–[152]. For example, Tanida *et al.* [151] introduce a Region-Guided Radiology Report Generation method that identifies unique anatomical regions in the chest and generates specific descriptions for the most salient areas, ensuring each sentence in the report is linked to a particular anatomical region. Overall, semi-structured approaches effectively balance the rigidity of fully structured reports with the inconsistency of completely free-text reports.

3) *Free-structured text generation*: With the advancement of language models, reports generated for a given input image are no longer limited to structured formats; instead, they now focus on more open, free-structured text descriptions. These approaches typically combine an image encoder to extract visual features with a language model to produce coherent sentences [153]. Several research efforts provide comprehensive explanations that include both textual and visual justifications for diagnostic decisions [154]–[157].

In addition to directly generating textual explanations, some research studies have incorporated the classification of pathological terms or tags in two distinct ways. The first approach utilizes a “classification-report generation” pipeline, integrating a classifier within the report generation network to enhance feature representations [158], [159]. For example, Yuan *et al.* [158] further employ a sentence-level attention mechanism alongside a word-level attention model to analyze multi-view chest X-rays, using predicted medical concepts to improve the accuracy of medical reports. Conversely, the second approach follows a “report generation-classification” pipeline, leveraging interpretable region-of-interest characterization for final diagnoses. For instance, Zhang *et al.* [160] construct a pathologist-level interpretable diagnostic framework that first detects tumour regions in whole slide images (WSIs), then generates natural language descriptions of microscopic findings with feature-aware visual attention, and finally establishes a diagnostic conclusion. Moreover, integrating region localization and lesion segmentation can enhance the quality of textual explanations [161]–[164]. For instance, Wang *et al.* [161] develop a Text-Image Embedding network that incorporates multi-level attention to highlight meaningful text words and X-ray image regions for disease detection and reporting.

The emergence of LLMs and VLMs offers a more in-

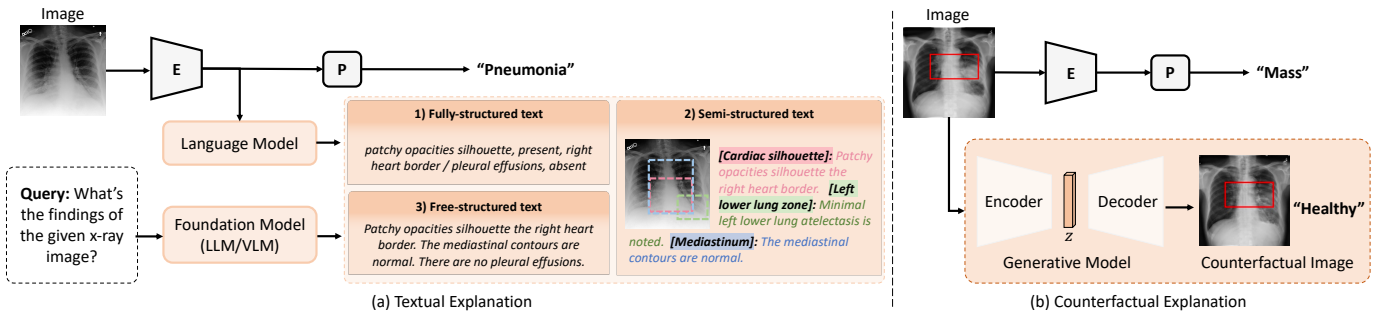


Fig. 8. Output explainability that provides (a) textual explanations, including fully-structured, semi-structured, and free-structured text; and (b) counterfactual explanations. The difference (red box) indicates the explanation. X-ray images borrowed from [138].

teractive and comprehensible method for generating textual explanations. Recent medical VLMs applied to various medical images, such as chest X-rays (e.g., XrayGPT [165]), skin images (e.g., SkinGPT [166]), and general medical images (e.g., Med-flamingo [167], LLaMa-Med [168], MedDr [169], HuatuoGPT-Vision [170]), can analyze and respond to open-ended questions about the input images, thanks to their pretraining on extensive datasets of image-report pairs. Take XrayGPT [165] as an example, given an input image, this combined model can address open-ended questions, such as “What are the main findings and impressions from the given X-ray?”. These models not only excel in report generation, but also demonstrate exceptional capability in delivering comprehensive explanations for a wide range of medical inquiries.

Discussion: Textual explanations have demonstrated significant effectiveness in providing human-interpretable judgments through natural language. This type of S-XAI approach has become especially valuable with the advancement of language models, enabling the generation of lengthy reports and the ability to answer open-ended questions. However, it is crucial to enhance the quality and reliability of these generated textual explanations. Some recent studies utilize techniques such as knowledge decoupling [171] and instruction tuning [172] to address challenges like hallucination, thereby improving the effectiveness and trustworthiness of textual explanations.

B. Counterfactual Explanation

Counterfactual explanations describe a causal situation by imagining a hypothetical reality that contradicts the observed facts: *If X had not occurred, Y would not have occurred* [23]. These explanations present a contrastive example: for a given image, its counterfactual image can alter the model’s prediction to a predefined output through the minimal perturbation to observations on the original image, as illustrated in the diagram of Fig. 8(b). Traditional counterfactual explanations are generated through a post-hoc paradigm [173], that is, a classification model is first trained as a black-box model, and then a generative model such as GAN [174] is applied to produce the counterfactual counterpart. However, post-hoc counterfactual explanations are susceptible to issues related to the classifier’s robustness and complexity (e.g., overfitting and excessive generalization), resulting in explanations that are inadequate for effective interpretability [175].

To tackle this issue, some research has investigated self-explainable variants of counterfactual explanations. An al-

ternative is to incorporate a generative model directly into the predictor, training them jointly so that the model can generate explanations for its own predictions. For example, CounterNet [176] combines the training of the predictive model with the generation of counterfactual explanations in an end-to-end framework. Compared to post-hoc approaches, it is able to produce counterfactuals with higher validity. Similarly, VCNet *et al.* [177] utilizes a counterfactual generator based on a conditional variational autoencoder, allowing for control and adjustments in the latent space to create more realistic counterfactuals. In the medical field, Wilms *et al.* [178] introduce an invertible, self-explainable generative model based on efficient normalizing flow for brain age regression and brain sex classification on 3D neuroimaging data. This model can generate predictions during the forward process and produce explanations, including voxel-level attribution maps and counterfactual images, in the reverse process.

Discussion: S-XAI models that generate counterfactual explanations alongside predictions show greater promise than post-hoc methods. However, their application in medical image analysis remains largely underexplored.

VI. EVALUATION

Assessing explainability presents significant challenges. In this section, we will outline the desired characteristics and evaluation methods for explainability.

A. Desired Characteristics of Explainability

It is important for S-XAI models to possess certain desirable qualities when providing explanations. In medical applications, the characteristics of high-quality explanations should align closely with the real-world necessities of clinical practice. Van *et al.* [19] and Adadi *et al.* [184] summarize several essential traits of XAI methods for medical image analysis and healthcare, respectively. Jin *et al.* [181] propose five criteria for optimizing clinical XAI. With the development of LLMs, usability has emerged as a key factor that enhances a model’s credibility [185], with interactive and dynamic explanations being preferred over static ones. Table I presents expected traits based on our literature review regarding explanations and explainability methods.

B. Evaluation Methods

Doshi-Velez and Kim [186] propose three distinct categories for evaluating XAI methods. 1) Application-grounded

TABLE I
DESIRABLE CHARACTERISTICS OF EXPLANATIONS AND EXPLAINABILITY METHODS.

Type	Characteristic	Description	Ref.
<i>Explanations</i>	Faithfulness, Fidelity, Truthfulness	Explanations should truthfully reflect the AI model decision process.	[179]–[181]
	Consistency, Invariance, Robustness	For a fixed model, explanation of similar data points (with similar prediction outputs) should be similar.	[7], [181], [182]
	Understandability, Comprehensibility	Explanations should be easily understandable by clinical users without requiring technical knowledge.	[179], [181], [182]
	Clinical Relevance	Explanation should be relevant to physicians’ clinical decision-making pattern, and can support their clinical reasoning process.	[181]
	Plausibility, Factuality, Persuasiveness	Users’ judgment on explanation plausibility (i.e., how convincing the explanations are to humans) may inform users about AI decision quality, including potential flaws or biases.	[7], [179], [181]
<i>Explainability Methods</i>	Computational Complexity	The computational complexity of explanation algorithms.	[181], [183]
	Generalizability, Portability	To increase the utility because of the diversity of model architectures.	[183]

evaluations engage experts specific to a field to evaluation explanation quality. 2) Human-grounded evaluations involve non-experts assessing the overall quality of explanations. 3) Functionality-grounded evaluations use proxy tasks instead of human. In the medical field, it is crucial to involve domain experts in the evaluation process, ideally in contexts that utilize real tasks and data [2].

1) *Human-centered evaluation*: Conducting human-centered evaluations with medical experts is crucial to determine user satisfaction with the explanations provided by S-XAI models. These evaluations can assess explanation quality using both qualitative and quantitative metrics.

Qualitative metrics include evaluating the usefulness, satisfaction, confidence, and trust in provided explanations through interviews or questionnaires [187]. For instance, the System Causability Scale [188] can be used to measure the quality of interpretability methods applicable in the medical field. Gale *et al.* [141] assess experts’ acceptance of explanations by scoring each type on a 10-level Likert scale.

Quantitative metrics focus on measuring task performance of human-machine collaboration with factors such as accuracy, response time, likelihood of deviation, ability to detect errors, and even physiological responses [187]. For example, Sayres *et al.* [189] demonstrate that AI assistance improves diagnostic accuracy, subjective confidence, and time spent, based on investigations involving ten ophthalmologists with varying experience levels in grading diabetic retinopathy.

Overall, human-centered evaluations offer the significant advantage of providing direct and compelling evidence of the effectiveness of explanations [186]. However, they can be costly and time-consuming, as they require recruiting expert participants and obtaining necessary approvals. Most importantly, these evaluations are inherently subjective.

2) *Functionality-grounded evaluation*: This category of evaluation can be employed to assess the fidelity of explanations. The accuracy of S-XAI methods in generating genuine explanations is referred to as the fidelity of an explainer. We will present a variety of functionality-grounded evaluation methods for different types of explanations.

Attention-based explanations can be assessed through causal metrics in the absence of references, such as deletion

and insertion [190] and RemOve And Retrain (ROAR) [191]. They can also be evaluated by comparing with ground truth annotations such as semantic masks [73], [192] or human expert eye fixation [193]. Additionally, the Activation Precision metric [194] is introduced to quantify the proportion of relevant information from the relevant region used to classify the mass margin based on radiologist annotations.

Concept-based explanations can primarily be evaluated using metrics Concept Error [80], [102], T-CAV score [9], Completeness Score [195], and Concept Relevance [4], [84]. Other evaluation methods include Concept Alignment Score, Mutual Information [85], and Concept Purity [119].

Prototype-based explanations can be measured by non-representativeness (i.e., how well the examples represent the explanations) and diversity (i.e., the degree of integration within the explanation) [196]. Additionally, a consistency score and a stability score are also used to assess prototype-based explanations [133].

Textual explanations assessments involve using metrics such as BLEU [197], ROUGE-L [198], and CIDEr [199] to compare generated natural language descriptions against ground truth reference sentences provided by experts. A benchmark study [17] of textual explanations is conducted on chest X-ray image datasets.

Counterfactual explanations can be evaluated by counterfactual validity, proximity, sparsity, and diversity [200]. Other metrics include Frechet Inception Distance score, Foreign Object Preservation score, as well as clinical metrics to illustrate the clinical utility of explanations [201].

VII. CHALLENGES AND FUTURE DIRECTIONS

Despite the rapid advancements in S-XAI for medical image analysis, several significant challenges remain unresolved. In this section, we will analyze the existing challenges and discuss potential future directions to enhance the effectiveness and reliability of S-XAI in the medical domain.

A. Benchmark Construction

Establishing benchmarks for S-XAI in medical image analysis is essential, which enables standardize evaluations and fair comparisons between different methods.

1) *Dataset*: A major challenge of dataset construction is the limited availability of doctors to annotate large-scale medical images, especially in S-XAI, which requires fine-grained annotations such as concepts and textual descriptions. Current medical datasets that meet interpretability standards often have limited volumes, reducing the generalizability and applicability of S-XAI methods in real-world contexts.

2) *Evaluation*: Automated evaluation of explanations poses another significant challenge. In the medical field, human-centered evaluations often depend on clinician expertise, but variability in expert opinions can lead to biased and subjective assessments [202]. Additionally, existing functionality-grounded evaluations still rely on manual annotations.

To tackle these challenges, future directions include leveraging semi-automated annotation tools to assist clinicians in the annotation process, thereby reducing their workload. Furthermore, developing objective metrics and standardized protocols to assess the quality of model explanations will be a critical research trend in S-XAI.

B. S-XAI in the Era of Foundation Models

Medical foundation models, such as LLMs [203]–[205] and VLMs [165], [167], [206], are trained on extensive medical corpora, allowing them to inherently encode rich domain-specific knowledge. The convergence of S-XAI with these large models creates substantial opportunities for developing trustworthy medical AI systems in the future [185].

1) *S-XAI benefits foundation models*: Foundation models are typically large, with an enormous number of parameters, making it challenging to explore their decision-making processes. This complexity can lead to potential biases and a lack of transparency. In addition to using post-hoc techniques [207], [208] to interpret foundation models, S-XAI methods can enhance input explainability through explainable prompts [209] and knowledge-enhanced prompts [210].

2) *Foundation models advance S-XAI*: Foundation models learn useful representations from the clinical knowledge in medical corpora [211]. By leveraging their advanced capabilities, S-XAI methods can generate user-friendly explanations [212] and enable flexible generative concept-based learning [213]. Additionally, foundation models can aid in evaluating S-XAI methods that mimic human cognitive processes [214].

C. S-XAI with Human-in-the-loop

Integrating Human-in-the-loop (HITL) processes is crucial for effectively implementing S-XAI in the medical field. This approach not only enhances the overall performance of AI systems but also fosters trust among medical experts.

1) *Improving accuracy through human intervention*: A HITL framework allows for the identification and removal of potential confounding factors, such as artifacts or biases in datasets. For instance, clinicians can adjust predicted concepts, leading to a more accurate concept bottleneck model [90]. This collaborative approach significantly enhances the prediction accuracy by incorporating expert insights.

2) *Enhancing explainability through human feedback*: To ensure continuous improvement, a versioning or feedback evaluation system should be established, to build trust during hospital evaluations. This requires fostering collaboration between

S-XAI researchers and clinical practitioners to systematically gather and utilize feedback for model refinement.

A challenge in integrating HITL processes is the variability in clinician expertise and availability, which can impact the consistency and quality of feedback. Ensuring effective integration of human knowledge into the AI training process without introducing biases or errors is a complex task.

D. Trade-off between Performance and Interpretability

It is commonly believed that as model complexity increases to boost performance, interpretability tends to decline [215], [216]. Conversely, more interpretable models may sacrifice prediction accuracy. However, some researchers argue that *there is no scientific evidence for a general trade-off between accuracy and interpretability* [217]. Recent advancements in concept-based models [95], [96], [100] have shown performance comparable to black-box models in medical image analysis. This success relies on the ability to identify patterns in an interpretable way while accurately fitting the data [13]. Future S-XAI methods are expected to optimize both performance and interpretability, potentially establishing a theoretical foundation for this balance.

E. Other Explainability of S-XAI

1) *Multi-modal explainability*: Medical data often exists in various forms, such as images, texts, and omics. By integrating these modalities, multi-modal S-XAI methods can provide more comprehensive explanations that align with clinicians' processes. Additionally, S-XAI methods can be used to identify correlations during multi-modal data fusion [218], offering significant potential for discovering new biomarkers.

2) *Causal explainability*: Another direction for S-XAI focuses on causality, which defines the cause-and-effect relationship and can be mathematically modeled [219]. Traditional deep learning methods in medical imaging often confuse correlation with causation, leading to potentially harmful errors. For instance, DeGrave *et al.* [220] found that COVID-19 diagnosis methods are primarily identifying spurious correlations using XAI techniques. Several efforts [221], [222] have been made to address dataset biases, which would be highly beneficial.

VIII. CONCLUSION

This survey reviews recent advancements in self-explainable artificial intelligence (S-XAI) for medical image analysis. Contrary to previous surveys that primarily focus on post-hoc XAI techniques, this paper emphasizes inherently interpretable S-XAI models, which are gaining traction in research. This survey introduces S-XAI from three key perspectives, i.e., input explainability, model explainability, and output explainability. Additionally, this survey explores the desired characteristics of explainability and various evaluation methods for assessing explanation quality. While significant progress has been made, it also highlights key challenges that need to be tackled and provides insights for future research on trustworthy AI systems in clinical practice. Overall, this survey serves as a valuable reference for the XAI community, particularly within the medical imaging field, and lays the groundwork for future advancements that will improve the transparency and trustworthiness of AI tools in healthcare.

APPENDIX

A. Lists of reviewed S-XAI methods

We provide comprehensive lists of our reviewed S-XAI methods for medical image analysis, including knowledge graph (Table II), attention-based learning (Table III), concept-based learning (Table IV), prototype-based learning (Table V), and textual explanation (Table VI). Each table contains the information of the S-XAI technique employed, publication year, anatomical location, image modality, medical application, and the used datasets.

B. Public datasets used in S-XAI

We provide an overview of more than 70 datasets currently available for S-XAI in the medical image domain. Table VII presents the key characteristics of these datasets, including modality, scale, and task. In this section, we will introduce the relevant datasets categorized by image modalities, highlighting their contributions to the development of S-XAI. For more detailed information about these datasets, we direct readers to the relevant publications and sources.

1) *Radiology*: Radiological images generally include modalities such as X-ray, MRI, CT, mammography, and ultrasound. Among these, X-ray is one of the most commonly used modalities in S-XAI for medical image analysis. For instance, the SLAKE [41] dataset collects knowledge triplets from the open source knowledge graph to assist the model in achieving a better understanding of X-ray images. Medical-CXR-VQA [60] focuses on the five types of questions (i.e., *abnormality*, *presence*, *view*, *location* and *type*) and aligns them with the key information of the X-ray image, resulting more reliable answers. VQA-RAD [290] is manually constructed based on clinicians asking naturally occurring questions about radiology images and providing reference answers, resulting in a dataset rich in quality expertise and knowledge to capture the details of radiology images. OAI [258] provides knee X-rays for knee osteoarthritis grading and offers clinical concepts (e.g., joint space narrowing, bone spurs, calcification), making it suitable for concept-based learning. Moreover, datasets such as IU X-ray [225], MIMIC-CXR [226], OpenI [275], and Chest ImaGenome [293] provide a large number of chest X-rays along with corresponding free-text reports, which can facilitate the generation of textual explanations. Finally, MIMIC-CXR-VQA [292], CheXbench [172], SLAKE [41], and MIMIC-Diff-VQA [59] are constructed for the VQA task, providing support for interactive explanations of S-XAI models.

Regarding MRI, SUN09 [252] and AC17 [253] provide cardiac segmentation masks, while BraTS 2020 [255] offers brain masks. However, most MRI datasets have a limited number of samples, which may affect the generalization ability of models. For CT images, datasets like CT-150 [232], NIH-TCIA CT-82 [233], and LiTS [287] can be used for segmentation tasks, while LIDC-IDRI [272] provides lung cancer annotations with grade of eight attributes, benefiting concept-based learning. Additionally, disease diagnoses on mammography datasets

[229], [278], [294] and ultrasound datasets [271], [282] also serve as applications for S-XAI methods.

2) *Dermatology*: In the scope of dermatology, datasets with fine-grained concept annotations are commonly used in concept-based learning for S-XAI. Derm7pt [259] is a dermoscopic image dataset containing 1,011 images with clinical concepts for melanoma skin lesions according to the 7-point checklist criteria [295]. PH² dataset [260] includes 200 dermoscopic images of melanocytic lesions with segmentation masks and several clinical concepts. SkinCon [261] is a skin disease dataset containing 3,230 images with 48 clinical concepts densely annotated by dermatologists for fine-grained model debugging and analysis, where the images are selected from the Fitzpatrick 17k [264] and DDI [265] skin image datasets. Other datasets such as ISIC [236], [250], [257] and HAM10000 [254] are also broadly used datasets but without explicit fine-grained concept annotations. Dermoscopic image datasets significantly facilitate the development of S-XAI, however, annotating concept labels requires the efforts of human experts and is labor-intensive. Hence there are currently only a few datasets with a limited number of samples that have fine-grained concept labels. This poses a significant challenge for concept-based S-XAI, especially in supervised concept learning.

3) *Pathology*: With regard to pathological image datasets, PathVQA [223] is the first dataset focused on pathology VQA, featuring over 32K open-ended questions derived from 4,998 pathology images. PEIR Gross [286] contains 7,442 image-caption pairs across 21 different sub-categories, with each caption consisting of a single sentence. The Cancer Genome Atlas (TCGA) [228] provides multimodal data for over 20,000 tumor and normal samples, offers multimodal data for more than 20K tumor and normal samples, encompassing clinical data, DNA, and various imaging types (diagnostic images, tissue images, and radiological images). Additionally, datasets such as BACH [248], Biopsy4Grading [251], and NCT [269] are available for classifying breast cancer, non-alcoholic fatty liver disease, and colorectal cancer, respectively. WBCAtt [266] provides 113K microscopic images of white blood cells, annotated with 11 morphological attributes categorized into four main groups: overall cell, nucleus, cytoplasm, and granules. Since pathological images are the “gold standard” for cancer diagnosis, the development of S-XAI models in pathology is highly significant.

4) *Retinal images*: Regarding retinal disease classification, EyePACS [283] is a large-scale dataset for grading diabetic retinopathy, containing more than 88K images. ACRIMA [230] offers 705 images for glaucoma assessment. In addition to classification labels, FGADR [267], DDR [268], and IDRID [270] also provide fine-grained masks for segmenting various types of lesions.

5) *Others*: Other medical datasets utilized in S-XAI include the Hyperkvasir endoscopy dataset [296] and the Infectious Keratitis slit lamp microscopy dataset [273]. Additionally, recent datasets like PMC-OA [289] and PMC-VQA [291] collect data from open-source medical literature corpus. These datasets encompass a wealth of multimodal data, which significantly facilitate the development of medical foundation

TABLE II

INPUT EXPLAINABILITY METHODS BASED ON KNOWLEDGE GRAPH (KG). THE ABBREVIATIONS HERE ARE CLS: CLASSIFICATION, DET: DETECTION, MRG: MEDICAL REPORT GENERATION, VQA: VISUAL QUESTION ANSWERING.

Method	Year	Location	Modality	Task	Dataset	KG Type
Naseem <i>et al.</i> [36]	2023	Multiple	Pathology	VQA	[223]	Prior KG
Guo <i>et al.</i> [37]	2022	Multiple	X-ray, CT, MRI	VQA	[41]	Prior KG
Zhang <i>et al.</i> [38]	2020	Chest	X-ray	MRG	[224]	Prior KG
Liu <i>et al.</i> [39]	2021	Chest	X-ray	MRG	[225], [226]	Prior KG
Huang <i>et al.</i> [40]	2023	Chest	X-ray	MRG	[225], [226]	Prior KG
Liu <i>et al.</i> [41]	2021	Multiple	X-ray, CT, MRI	VQA	[41]	Prior KG
Chen <i>et al.</i> [45]	2020	Chest	X-ray	CLS	[224], [227]	Data KG
Hou <i>et al.</i> [46]	2021	Chest	X-ray	CLS	[225], [226]	Data KG
Liu <i>et al.</i> [47]	2021	Chest	X-ray	MRG	[225], [226]	Data KG
Huang <i>et al.</i> [48]	2023	Multiple	X-ray, CT, MRI, US	VQA	[41]	Data KG
Li <i>et al.</i> [49]	2024	Multiple	Pathology	CLS	[228]	Data KG
Zheng <i>et al.</i> [50]	2021	Chest	X-ray, CT, US, text	CLS	private	Data KG
Liu <i>et al.</i> [51]	2021	Breast	Mammogram	DET	[229]	Data KG
Zhao <i>et al.</i> [52]	2021	Chest	X-ray	DET	[224]	Data KG
Qi <i>et al.</i> [53]	2022	Chest	X-ray	DET	[224]	Data KG
Zhou <i>et al.</i> [54]	2021	Chest	X-ray	CLS	[224], [227]	Hybrid KG
Wu <i>et al.</i> [55]	2023	Chest	X-ray	CLS	[226]	Hybrid KG
Li <i>et al.</i> [56]	2019	Chest	X-ray	MRG	[225]	Hybrid KG
Li <i>et al.</i> [57]	2023	Chest	X-ray	MRG	[225], [226]	Hybrid KG
Kale <i>et al.</i> [58]	2023	Chest	X-ray	MRG	[225]	Hybrid KG
Hu <i>et al.</i> [59]	2023	Chest	X-ray	VQA	[59]	Hybrid KG
Hu <i>et al.</i> [60]	2024	Chest	X-ray	VQA	[59]	Hybrid KG

TABLE III

MODEL EXPLAINABILITY METHODS BASED ON ATTENTION-BASED LEARNING. THE ABBREVIATIONS HERE ARE CLS: CLASSIFICATION, SEG: SEGMENTATION, IRE: IMAGE RECONSTRUCTION, REG: REGRESSION.

Method	Year	Location	Modality	Task	Dataset	Attention Type
Li <i>et al.</i> [65]	2021	Eye	Retinal images	CLS	[230]	Structure-Guided
Wang <i>et al.</i> [66]	2018	Breast	X-ray	CLS	[231]	Structure-Guided
Schempler <i>et al.</i> [67]	2019	Abdominal, Fetal	CT, US	SEG + DET	[232], [233]	Structure-Guided
Lian <i>et al.</i> [68]	2019	Brain	MRI	REG	[234], [235]	Structure-Guided
Gu <i>et al.</i> [69]	2020	Skin, Fetal	Dermatology, MRI	SEG	[236]	Structure-Guided
Lozupone <i>et al.</i> [70]	2024	Brain	MRI	CLS	[234]	Structure-Guided
Huang <i>et al.</i> [71]	2022	Head	MRI	IRE	[237]	Structure-Guided
Bhattacharya <i>et al.</i> [62]	2022	Chest	X-ray	CLS	[238]–[247]	Loss-Guided
Yang <i>et al.</i> [72]	2019	Breast	Histopathology	CLS	[248]	Loss-Guided
Yan <i>et al.</i> [73]	2019	Skin	Dermatology	CLS	[249], [250]	Loss-Guided
Barata <i>et al.</i> [74]	2021	Skin	Dermatology	CLS	[250], [236]	Loss-Guided
Yin <i>et al.</i> [75]	2021	Liver	Histopathology	CLS	[251]	Loss-Guided
Sun <i>et al.</i> [76]	2020	Cardiac	MRI	SEG	[252], [253]	Loss-Guided
Karri <i>et al.</i> [77]	2022	Skin, Brain, Abdominal	Dermatology, MRI, CT	SEG	[254]–[256]	Loss-Guided
Li <i>et al.</i> [78]	2023	Skin	Dermatology	SEG	[236], [250], [254], [257]	Loss-Guided

TABLE IV

MODEL EXPLAINABILITY METHODS BASED ON CONCEPT-BASED LEARNING. THE ABBREVIATIONS HERE ARE CLS: CLASSIFICATION.

Method	Year	Location	Modality	Task	Dataset	Concept
Koh <i>et al.</i> [80]	2020	Knee	X-ray	CLS	[258]	Supervised (CBM)
Chauhan <i>et al.</i> [88]	2023	Knee, Chest	X-ray	CLS	[258], [227]	Supervised (CBM)
Patricio <i>et al.</i> [89]	2023	Skin	Dermatology	CLS	[259], [260]	Supervised (CBM)
Yan <i>et al.</i> [90]	2023	Skin	Dermatology	CLS	Private	Supervised (CBM)
Bie <i>et al.</i> [91]	2024	Skin	Dermatology	CLS	[259]–[261]	Supervised (CBM)
Marcinkevics <i>et al.</i> [92]	2024	Appendix	US	CLS	Private	Supervised (CBM)
Lucieri <i>et al.</i> [93]	2022	Skin	Dermatology	CLS	[259], [260], [257]	Supervised
Jalaboi <i>et al.</i> [94]	2023	Skin	Dermatology	CLS	[262], [263]	Supervised
Kim <i>et al.</i> [95]	2024	Skin	Dermatology	CLS	[257], [259], [261], [264], [265]	Supervised (CBM)
Pang <i>et al.</i> [96]	2024	Skin, Blood cell	Dermatology, Microscopy	CLS	[261], [266]	Supervised (CBM)
Wen <i>et al.</i> [97]	2024	Eye	Retinal images	CLS	[267], [268]	Supervised
Gao <i>et al.</i> [98]	2024	Multiple	Dermatology, Pathology, US, X-ray	CLS	[226], [254], [269]–[271]	Supervised
Hou <i>et al.</i> [100]	2024	Skin	Dermatology	CLS	[259], [261]	Supervised
Zhao <i>et al.</i> [101]	2021	Chest	CT	CLS	[272]	Supervised
Fang <i>et al.</i> [103]	2020	Eye	Slit lamp microscopy	CLS	[273]	Concept discovery
Kim <i>et al.</i> [108]	2023	Skin	Dermatology	CLS	[254]	Generated concept
Liu <i>et al.</i> [109]	2023	Multiple	X-ray, CT	CLS	[239], [270], [274]	Generated concept
Patricio <i>et al.</i> [110]	2024	Skin	Dermatology	CLS	[259], [260], [236]	Generated concept
Bie <i>et al.</i> [111]	2024	Multiple	Dermatology, X-ray	CLS	[239], [259], [261], [275]	Generated concept

TABLE V

MODEL EXPLAINABILITY METHODS BASED ON PROTOTYPE-BASED LEARNING. THE ABBREVIATIONS HERE ARE CLS: CLASSIFICATION, REG: REGRESSION.

Method	Year	Location	Modality	Task	Dataset	Prototype Type
Kim <i>et al.</i> [112]	2020	Chest	X-ray	CLS	[224]	Explicit
Singh <i>et al.</i> [123]	2021	Chest	X-ray	CLS	[276]	Explicit
Mohammadjafari <i>et al.</i> [124]	2021	Brain	MRI	CLS	[277]	Explicit
Carloni <i>et al.</i> [125]	2022	Breast	Mammogram	CLS	[278]	Explicit
Wang <i>et al.</i> [126]	2022	Breast	Mammogram	CLS	[279]	Explicit
Barnett <i>et al.</i> [127]	2021	Breast	Mammogram	CLS	Private	Explicit
Wei <i>et al.</i> [128]	2024	Brain	MRI	CLS	[280]	Explicit
Hesse <i>et al.</i> [129]	2024	Brain	MRI, US	REG	[281], [282]	Explicit
Hesse <i>et al.</i> [130]	2022	Eye	Retinal images	REG	[283]	Explicit
Santos <i>et al.</i> [131]	2024	Eye	Retinal images	CLS	[284]	Explicit

TABLE VI

OUTPUT EXPLAINABILITY METHODS THAT PROVIDE TEXTUAL EXPLANATIONS. THE ABBREVIATIONS HERE ARE MRG: MEDICAL REPORT GENERATION, CLS: CLASSIFICATION, LOC: LOCATION, SEG: SEGMENTATION, VQA: VISUAL QUESTION ANSWERING, VIS: VISUAL EXPLANATION.

Method	Year	Location	Modality	Task	Dataset	Text Type	Vis.
Pino <i>et al.</i> [139]	2021	Chest	X-ray	MRG	[225], [226]	Fully-structured	✓
Rodin <i>et al.</i> [140]	2019	Chest	X-ray	MRG	[226]	Fully-structured	✓
Gale <i>et al.</i> [141]	2019	Pelvic	X-ray	MRG	Private	Fully-structured	✓
Shin <i>et al.</i> [143]	2016	Chest	X-ray	CLS + MRG	[275]	Fully-structured	-
Gasimova <i>et al.</i> [144]	2019	Chest	X-ray	CLS + MRG	[275]	Fully-structured	-
Zhang <i>et al.</i> [145]	2017	Bladder	Pathology	MRG	Private	Semi-structured	✓
Zhang <i>et al.</i> [146]	2017	Bladder	Pathology	MRG	Private	Semi-structured	✓
Ma <i>et al.</i> [147]	2018	Cervix	Pathology	MRG	Private	Semi-structured	✓
Wang <i>et al.</i> [148]	2019	Chest	X-ray	CLS + MRG	[225]	Semi-structured	✓
Tanida <i>et al.</i> [151]	2023	Chest	X-ray	LOC + MRG	[149]	Semi-structured	✓
Wang <i>et al.</i> [152]	2022	Chest	X-ray	CLS + MRG	[225], [226]	Semi-structured	-
Singh <i>et al.</i> [153]	2019	Chest	X-ray	MRG	[225]	Free-structured	-
Spinks <i>et al.</i> [154]	2019	Chest	X-ray	MRG	[225], [285]	Free-structured	✓
Liu <i>et al.</i> [155]	2019	Chest	X-ray	MRG	[225], [226]	Free-structured	✓
Chen <i>et al.</i> [156]	2020	Chest	X-ray	MRG	[225], [226]	Free-structured	✓
Wang <i>et al.</i> [157]	2023	Chest	X-ray	MRG	[225], [226]	Free-structured	✓
Yuan <i>et al.</i> [158]	2019	Chest	X-ray	CLS + MRG	[225], [227]	Free-structured	✓
Lee <i>et al.</i> [159]	2019	Breast	Mammogram	CLS + MRG	[229]	Free-structured	✓
Zhang <i>et al.</i> [160]	2019	Bladder	Pathology	CLS + MRG	[228]	Free-structured	✓
Wang <i>et al.</i> [161]	2018	Chest	X-ray	LOC + MRG	[224], [275]	Free-structured	✓
Jing <i>et al.</i> [162]	2018	Multiple	X-ray, Pathology	LOC + MRG	[225], [286]	Free-structured	✓
Zeng <i>et al.</i> [163]	2020	Multiple	US, X-ray	LOC + MRG	[275]	Free-structured	✓
Tian <i>et al.</i> [164]	2018	Abdomen	CT	SEG + MRG	[287]	Free-structured	✓
Thawkar <i>et al.</i> [165]	2023	Chest	X-ray	VQA	[226]	Free-structured	-
Zhou <i>et al.</i> [166]	2024	Skin	Dermatology	VQA	[261], [288]	Free-structured	-
Moor <i>et al.</i> [167]	2023	Multiple	Multiple	VQA	[289]	Free-structured	-
Li <i>et al.</i> [168]	2024	Multiple	Multiple	VQA	[41], [223], [290]	Free-structured	-
He <i>et al.</i> [169]	2024	Multiple	Multiple	VQA	[223], [226], [290]	Free-structured	-
Chent <i>et al.</i> [170]	2024	Multiple	Multiple	VQA	[41], [223], [290], [291]	Free-structured	-
Kang <i>et al.</i> [171]	2024	Chest	X-ray	VQA	[225], [226], [292]	Free-structured	-
Chen <i>et al.</i> [172]	2024	Chest	X-ray	VQA	[172]	Free-structured	-

models.

TABLE VII: Public datasets used in the reviewed S-XAI methods.

Dataset	Modality	Scale	Task
SLAKE [41]	X-ray	642 images, 14,028 QA pairs	VQA, SEG, DET
ChestXray [224]	X-ray	108,948 images	CLS, MRG, DET, LOC
IU X-ray [225]	X-ray	8,121 images, 3,996 texts	MRG
MIMIC-Diff-VQA [59]	X-ray	700K QA pairs, 164K images	VQA
OAI [258]	X-ray	26,626,000 images	CLS
CheXbench [172]	X-ray	6.1M QA pairs	VQA
CheXpert [227]	X-ray	224K images	CLS
MIMIC-CXR [226]	X-ray	377K images, 227K texts	CLS, MRG
BCDR-F03 [231]	X-ray	736 images	CLS
RSNA [238]	X-ray	30,000 images	CLS, DET
ZhangLabData [239]	OCT, X-ray	108,312 OCT images, 5,232 X-ray images	CLS
SIIM-FISABIO-RSNA [240]	X-ray	10,178 images	CLS, DET
Public Radiography [241]	X-ray	3,487 images	CLS
COVQU [242]	X-ray	18,479 images	CLS, SEG
COVID-19-NY-SBU [243]	X-ray, CT, MRI	1,384 cases	CLS
MIDRC-RICORD-1C [244]	X-ray	361 cases	CLS
NIH [246]	X-ray	108,948 images	CLS
VinBigData [247]	X-ray	18,000 images	CLS, DET
Montgomery [274]	X-ray	138 images	CLS
COVID-19 [276]	X-ray	761 images	CLS
OpenI [275]	X-ray	7,470 images, 3,955 texts	CLS, MRG
Chest ImaGenome [149]	X-ray	242K images, 217K texts	CLS, MRG, DET
MIMIC-CXR-VQA [292]	X-ray	377K images with QA pairs	VQA
ADNI-1 [234]	MRI	818 subjects	CLS, REG
ADNI-2 [235]	MRI	599 subjects	CLS, REG
SUN09 [252]	MRI	395 slices	SEG
AC17 [253]	MRI	200 volumes	SEG
BraTS 2020 [255]	MRI	494 cases	SEG, CLS
Calgary Campinas MRI [237]	MRI	359 subjects	SEG
OASIS [277]	MRI	416 cases	CLS
BraTS 2014 [280]	MRI	65 scans	SEG
IXI [281]	MRI	600 cases	REG
RICODR [245]	CT, X-ray	240 CT scans, 1,000 X-ray images	CLS
CT-150 [232]	CT	150 scans	SEG
Pancreas-CT [233]	CT	82 scans	SEG
CHAOS [256]	CT, MRI	40 CT scans, 120 MRI scans	SEG
LIDC-IDRI [272]	CT	1,018 scans	CLS, SEG
LiTS [287]	CT	201 scans	SEG
VQA-RAD [290]	CT, MRI, X-ray	3,515 QA pairs, 315 images	VQA
DDSM [229]	Mammogram	2,620 cases	CLS, MRG, SEG
CBIS-DDSM [278]	Mammogram	1,644 cases	CLS, SEG
CMMD [279]	Mammogram	1,775 cases	CLS
BUSI [271]	Ultrasound	780 images	CLS
FGLS [282]	Ultrasound	4,290 volumes	REG
HAM10000 [254]	Dermatology	10,015 images	CLS
ISIC 2016 [249]	Dermatology	1,279 images	CLS, SEG
ISIC 2017 [250]	Dermatology	2,750 images	CLS, SEG
ISIC 2018 [236]	Dermatology	15,121 images	CLS, SEG
ISIC 2019 [257]	Dermatology	33,569 images	CLS
Derm7pt [259]	Dermatology	1,011 images	CLS
PH ² [260]	Dermatology	200 images	CLS, SEG
SkinCon [261]	Dermatology	3,230 images	CLS
Fitzpatrick 17k [264]	Dermatology	16,577 images	CLS
DDI [265]	Dermatology	656 images	CLS
DermNetNZ [262]	Dermatology	25K images	CLS
SD-260 [263]	Dermatology	6,584 images	CLS
Dermnet [288]	Dermatology	18,856 images	CLS, VQA
PathVQA [223]	Pathology	32K QA pairs, 4,998 images	VQA
BACH [248]	Histopathology	500 images	CLS
Biopsy4Grading [251]	Histopathology	351 images	CLS
WBCAtt [266]	Microscopy	113,278 images	CLS
NCT [269]	Histopathology	100K images	CLS
TCGA [228]	Pathology	20K studies	CLS, MRG
PEIR Gross [286]	Pathology	7,442 image-text pairs	MRG
ACRIMA [230]	Retinal images	705 images	CLS
FGADR [267]	Retinal images	2,842 images	CLS, SEG
DDR [268]	Retinal images	13,673 images	CLS, SEG, DET
IDRID [270]	Retinal images	516 images	CLS, SEG, LOC

Continued on next page

– continued from previous page

Dataset	Modality	Scale	Task
EyePACS [283]	Retinal images	88,702 images	CLS
Messidor [284]	Retinal images	1,200 images	CLS
Hyperkvasir [296]	Endoscopy	110,079 images, 374 videos	SEG, DET
Infectious Keratitis [273]	Slit lamp microscopy	115,408 images	CLS
PMC-OA [289]	Multiple	1.65M image-text pairs	VQA
PMC-VQA [291]	Multiple	227K QA pairs, 149K images	VQA

REFERENCES

- [1] X. Jia, L. Ren, and J. Cai, "Clinical implementation of ai technologies will require interpretable ai models," *Medical Physics*, no. 1, pp. 1–4, 2020.
- [2] Z. Salahuddin *et al.*, "Transparency of deep neural networks for medical image analysis: A review of interpretability methods," *Computers in Biology and Medicine*, vol. 140, p. 105111, 2022.
- [3] L. Luo *et al.*, "Rethinking annotation granularity for overcoming shortcuts in deep learning-based radiograph diagnosis: A multicenter study," *Radiology: Artificial Intelligence*, vol. 4, no. 5, p. e210299, 2022.
- [4] D. Alvarez Melis and T. Jaakkola, "Towards robust interpretability with self-explaining neural networks," *Advances in Neural Information Processing Systems (NeurIPS)*, vol. 31, 2018.
- [5] S. Bach *et al.*, "On pixel-wise explanations for non-linear classifier decisions by layer-wise relevance propagation," *PLoS one*, vol. 10, no. 7, p. e0130140, 2015.
- [6] B. Zhou *et al.*, "Learning deep features for discriminative localization," in *Proceedings of the IEEE Conference on Computer Vision and Pattern Recognition (CVPR)*, 2016, pp. 2921–2929.
- [7] M. T. Ribeiro, S. Singh, and C. Guestrin, "Why should i trust you? explaining the predictions of any classifier," in *Proceedings of the 22nd ACM SIGKDD International Conference on Knowledge Discovery and Data Mining (SIGKDD)*, 2016, pp. 1135–1144.
- [8] S. M. Lundberg and S.-I. Lee, "A unified approach to interpreting model predictions," *NeurIPS*, vol. 30, 2017.
- [9] B. Kim *et al.*, "Interpretability beyond feature attribution: Quantitative testing with concept activation vectors (tcav)," in *International Conference on Machine Learning (ICML)*. PMLR, 2018, pp. 2668–2677.
- [10] J. Crabbé and M. van der Schaar, "Concept activation regions: A generalized framework for concept-based explanations," *NeurIPS*, vol. 35, pp. 2590–2607, 2022.
- [11] B. Mittelstadt, C. Russell, and S. Wachter, "Explaining explanations in ai," in *Proceedings of the Conference on Fairness, Accountability, and Transparency (FAccT)*, 2019, pp. 279–288.
- [12] J. Zhang *et al.*, "Overlooked trustworthiness of saliency maps," in *International Conference on Medical Image Computing and Computer-Assisted Intervention (MICCAI)*. Springer, 2022, pp. 451–461.
- [13] C. Rudin, "Stop explaining black box machine learning models for high stakes decisions and use interpretable models instead," *Nature Machine Intelligence*, vol. 1, no. 5, pp. 206–215, 2019.
- [14] J. R. Quinlan, "Induction of decision trees," *Machine Learning*, vol. 1, pp. 81–106, 1986.
- [15] T. J. Hastie, "Generalized additive models," in *Statistical models in S*. Routledge, 2017, pp. 249–307.
- [16] C. Grosan and A. Abraham, *Intelligent Systems*. Springer, vol. 17.
- [17] C. Patrício, J. C. Neves, and L. F. Teixeira, "Explainable deep learning methods in medical image classification: A survey," *ACM Computing Surveys*, vol. 56, no. 4, pp. 1–41, 2023.
- [18] G. Yang, Q. Ye, and J. Xia, "Unbox the black-box for the medical explainable ai via multi-modal and multi-centre data fusion: A mini-review, two showcases and beyond," *Information Fusion*, vol. 77, pp. 29–52, 2022.
- [19] B. H. Van der Velden *et al.*, "Explainable artificial intelligence (xai) in deep learning-based medical image analysis," *Medical Image Analysis (MedIA)*, vol. 79, p. 102470, 2022.
- [20] R.-K. Sheu and M. S. Pardeshi, "A survey on medical explainable ai (xai): recent progress, explainability approach, human interaction and scoring system," *Sensors*, vol. 22, no. 20, p. 8068, 2022.
- [21] E. Tjoa and C. Guan, "A survey on explainable artificial intelligence (xai): Toward medical xai," *IEEE Transactions on Neural Networks and Learning Systems (TNNLS)*, vol. 32, no. 11, pp. 4793–4813, 2020.
- [22] A. Singh, S. Sengupta, and V. Lakshminarayanan, "Explainable deep learning models in medical image analysis," *Journal of Imaging*, vol. 6, no. 6, p. 52, 2020.
- [23] M. Christoph, *Interpretable machine learning: A guide for making black box models explainable*. Leanpub, 2020.
- [24] A. Zheng and A. Casari, *Feature engineering for machine learning: principles and techniques for data scientists*. O'Reilly Media, Inc., 2018.
- [25] S. Kapse *et al.*, "Si-mil: Taming deep mil for self-interpretability in gigapixel histopathology," in *CVPR*, 2024, pp. 11 226–11 237.
- [26] U. Sajid *et al.*, "Breast cancer classification using deep learned features boosted with handcrafted features," *Biomedical Signal Processing and Control*, vol. 86, p. 105353, 2023.
- [27] H. Xiang *et al.*, "Development and validation of an interpretable model integrating multimodal information for improving ovarian cancer diagnosis," *Nature Communications*, vol. 15, no. 1, p. 2681, 2024.
- [28] N. Lassau *et al.*, "Integrating deep learning ct-scan model, biological and clinical variables to predict severity of covid-19 patients," *Nature Communications*, vol. 12, no. 1, pp. 1–11, 2021.
- [29] A. Hogan *et al.*, "Knowledge graphs," *ACM Computing Surveys*, vol. 54, no. 4, pp. 1–37, 2021.
- [30] S. Ji *et al.*, "A survey on knowledge graphs: Representation, acquisition, and applications," *TNNLS*, vol. 33, no. 2, pp. 494–514, 2021.
- [31] C. Peng *et al.*, "Knowledge graphs: Opportunities and challenges," *Artificial Intelligence Review*, vol. 56, no. 11, pp. 13 071–13 102, 2023.
- [32] S. Pan *et al.*, "Unifying large language models and knowledge graphs: A roadmap," *IEEE Transactions on Knowledge and Data Engineering*, 2024.
- [33] X. Xie *et al.*, "A survey on incorporating domain knowledge into deep learning for medical image analysis," *MedIA*, vol. 69, p. 101985, 2021.
- [34] S. Liu and H. Chen, "Knowledge injected multimodal irregular ehcs model for medical prediction," in *International Workshop on Trustworthy Artificial Intelligence for Healthcare*. Springer, 2024, pp. 25–39.
- [35] S. Liu *et al.*, "Shape: A sample-adaptive hierarchical prediction network for medication recommendation," *IEEE Journal of Biomedical and Health Informatics (JBHI)*, 2023.
- [36] U. Naseem *et al.*, "K-pathvqa: Knowledge-aware multimodal representation for pathology visual question answering," *JBHI*, 2023.
- [37] H. Guo *et al.*, "Medical visual question answering via targeted choice contrast and multimodal entity matching," in *International Conference on Neural Information Processing (ICONIP)*. Springer, 2022, pp. 343–354.
- [38] Y. Zhang *et al.*, "When radiology report generation meets knowledge graph," in *Proceedings of the AAAI conference on Artificial Intelligence (AAAI)*, vol. 34, no. 07, 2020, pp. 12 910–12 917.
- [39] F. Liu *et al.*, "Exploring and distilling posterior and prior knowledge for radiology report generation," in *CVPR*, 2021, pp. 13 753–13 762.
- [40] Z. Huang, X. Zhang, and S. Zhang, "Kiut: Knowledge-injected u-transformer for radiology report generation," in *CVPR*, 2023, pp. 19 809–19 818.
- [41] B. Liu *et al.*, "Slake: A semantically-labeled knowledge-enhanced dataset for medical visual question answering," in *2021 IEEE 18th International Symposium on Biomedical Imaging (ISBI)*. IEEE, 2021, pp. 1650–1654.
- [42] L. Li *et al.*, "Real-world data medical knowledge graph: construction and applications," *Artificial Intelligence in Medicine*, vol. 103, p. 101817, 2020.
- [43] S. Liu *et al.*, "A hybrid method of recurrent neural network and graph neural network for next-period prescription prediction," *International Journal of Machine Learning and Cybernetics*, vol. 11, pp. 2849–2856, 2020.
- [44] X. Wu *et al.*, "Medical knowledge graph: Data sources, construction, reasoning, and applications," *Big Data Mining and Analytics*, vol. 6, no. 2, pp. 201–217, 2023.
- [45] B. Chen *et al.*, "Label co-occurrence learning with graph convolutional networks for multi-label chest x-ray image classification," *JBHI*, vol. 24, no. 8, pp. 2292–2302, 2020.
- [46] D. Hou, Z. Zhao, and S. Hu, "Multi-label learning with visual-semantic embedded knowledge graph for diagnosis of radiology imaging," *IEEE Access*, vol. 9, pp. 15 720–15 730, 2021.
- [47] F. Liu *et al.*, "Auto-encoding knowledge graph for unsupervised medical report generation," *NeurIPS*, vol. 34, pp. 16 266–16 279, 2021.
- [48] J. Huang *et al.*, "Medical knowledge-based network for patient-oriented visual question answering," *Information Processing & Management*, vol. 60, no. 2, p. 103241, 2023.
- [49] J. Li *et al.*, "Dynamic graph representation with knowledge-aware attention for histopathology whole slide image analysis," in *CVPR*, 2024, pp. 11 323–11 332.
- [50] W. Zheng *et al.*, "Pay attention to doctor-patient dialogues: Multimodal knowledge graph attention image-text embedding for covid-19 diagnosis," *Information Fusion*, vol. 75, pp. 168–185, 2021.
- [51] Y. Liu *et al.*, "Act like a radiologist: towards reliable multi-view correspondence reasoning for mammogram mass detection," *IEEE Transactions on Pattern Analysis and Machine Intelligence (TPAMI)*, vol. 44, no. 10, pp. 5947–5961, 2021.
- [52] G. Zhao, "Cross chest graph for disease diagnosis with structural relational reasoning," in *Proceedings of the 29th ACM International Conference on Multimedia (ACM MM)*, 2021, pp. 612–620.

- [53] B. Qi *et al.*, “Gren: graph-regularized embedding network for weakly-supervised disease localization in x-ray images,” *JBHI*, vol. 26, no. 10, pp. 5142–5153, 2022.
- [54] Y. Zhou *et al.*, “Contrast-attentive thoracic disease recognition with dual-weighting graph reasoning,” *IEEE Transactions on Medical Imaging (TMI)*, vol. 40, no. 4, pp. 1196–1206, 2021.
- [55] C. Wu *et al.*, “Medklip: Medical knowledge enhanced language-image pre-training for x-ray diagnosis,” in *Proceedings of the IEEE/CVF International Conference on Computer Vision (ICCV)*, 2023, pp. 21 372–21 383.
- [56] C. Y. Li *et al.*, “Knowledge-driven encode, retrieve, paraphrase for medical image report generation,” in *AAAI*, vol. 33, no. 01, 2019, pp. 6666–6673.
- [57] M. Li *et al.*, “Dynamic graph enhanced contrastive learning for chest x-ray report generation,” in *CVPR*, 2023, pp. 3334–3343.
- [58] K. Kale *et al.*, “Kgv1-bart: Knowledge graph augmented visual language bart for radiology report generation,” in *Proceedings of the 17th Conference of the European Chapter of the Association for Computational Linguistics*, 2023, pp. 3401–3411.
- [59] X. Hu *et al.*, “Expert knowledge-aware image difference graph representation learning for difference-aware medical visual question answering,” in *SIGKDD*, 2023, pp. 4156–4165.
- [60] X. Hu *et al.*, “Interpretable medical image visual question answering via multi-modal relationship graph learning,” *MedIA*, vol. 97, p. 103279, 2024.
- [61] Z. Niu, G. Zhong, and H. Yu, “A review on the attention mechanism of deep learning,” *Neurocomputing*, vol. 452, pp. 48–62, 2021.
- [62] M. Bhattacharya, S. Jain, and P. Prasanna, “Radiotransformer: a cascaded global-focal transformer for visual attention-guided disease classification,” in *European Conference on Computer Vision (ECCV)*. Springer, 2022, pp. 679–698.
- [63] S. Jetley *et al.*, “Learn to pay attention,” in *International Conference on Learning Representations (ICLR)*, 2018.
- [64] H. Fukui *et al.*, “Attention branch network: Learning of attention mechanism for visual explanation,” in *CVPR*, 2019, pp. 10705–10714.
- [65] L. Li *et al.*, “Scouter: Slot attention-based classifier for explainable image recognition,” in *ICCV*, 2021, pp. 1046–1055.
- [66] H. Wang *et al.*, “Breast mass classification via deeply integrating the contextual information from multi-view data,” *Pattern Recognition*, vol. 80, pp. 42–52, 2018.
- [67] J. Schlemper *et al.*, “Attention gated networks: Learning to leverage salient regions in medical images,” *MedIA*, vol. 53, pp. 197–207, 2019.
- [68] C. Lian *et al.*, “End-to-end dementia status prediction from brain mri using multi-task weakly-supervised attention network,” in *MICCAI*, 2019, pp. 158–167.
- [69] R. Gu *et al.*, “Ca-net: Comprehensive attention convolutional neural networks for explainable medical image segmentation,” *TMI*, vol. 40, no. 2, pp. 699–711, 2020.
- [70] G. Lozupone *et al.*, “Axial: Attention-based explainability for interpretable alzheimer’s localized diagnosis using 2d cnns on 3d mri brain scans,” *arXiv preprint arXiv:2407.02418*, 2024.
- [71] J. Huang *et al.*, “Swin deformable attention u-net transformer (sdaut) for explainable fast mri,” in *MICCAI*. Springer, 2022, pp. 538–548.
- [72] H. Yang *et al.*, “Guided soft attention network for classification of breast cancer histopathology images,” *TMI*, vol. 39, no. 5, pp. 1306–1315, 2019.
- [73] Y. Yan, J. Kawahara, and G. Hamarneh, “Melanoma recognition via visual attention,” in *Information Processing in Medical Imaging: 26th International Conference, IPMI 2019, Hong Kong, China, June 2–7, 2019, Proceedings 26*. Springer, 2019, pp. 793–804.
- [74] C. Barata, M. E. Celebi, and J. S. Marques, “Explainable skin lesion diagnosis using taxonomies,” *Pattern Recognition*, vol. 110, p. 107413, 2021.
- [75] C. Yin *et al.*, “Focusing on clinically interpretable features: Selective attention regularization for liver biopsy image classification,” in *MICCAI*, 2021, pp. 153–162.
- [76] J. Sun *et al.*, “Saunet: Shape attentive u-net for interpretable medical image segmentation,” in *MICCAI*, 2020, pp. 797–806.
- [77] M. Karri, C. S. R. Annavarapu, and U. R. Acharya, “Explainable multi-module semantic guided attention based network for medical image segmentation,” *Computers in Biology and Medicine*, vol. 151, p. 106231, 2022.
- [78] H. Li *et al.*, “Pmjaf-net: Pyramidal multi-scale joint attention and adaptive fusion network for explainable skin lesion segmentation,” *Computers in Biology and Medicine*, p. 107454, 2023.
- [79] E. Poeta *et al.*, “Concept-based explainable artificial intelligence: A survey,” *arXiv preprint arXiv:2312.12936*, 2023.
- [80] P. W. Koh *et al.*, “Concept bottleneck models,” in *ICML*. PMLR, 2020, pp. 5338–5348.
- [81] M. Yuksekgonul, M. Wang, and J. Zou, “Post-hoc concept bottleneck models,” in *ICLR*, 2023.
- [82] R. Jain *et al.*, “Extending logic explained networks to text classification,” *arXiv preprint arXiv:2211.09732*, 2022.
- [83] A. Tan, F. Zhou, and H. Chen, “Explain via any concept: Concept bottleneck model with open vocabulary concepts,” in *ECCV*, 2024.
- [84] R. Ahtibat *et al.*, “From attribution maps to human-understandable explanations through concept relevance propagation,” *Nature Machine Intelligence*, vol. 5, no. 9, pp. 1006–1019, 2023.
- [85] M. Espinosa Zarlenga *et al.*, “Concept embedding models: Beyond the accuracy-explainability trade-off,” *NeurIPS*, vol. 35, pp. 21 400–21 413, 2022.
- [86] P. Barbiero *et al.*, “Entropy-based logic explanations of neural networks,” in *AAAI*, vol. 36, no. 6, 2022, pp. 6046–6054.
- [87] H. Wang, J. Hou, and H. Chen, “Concept complement bottleneck model for interpretable medical image diagnosis,” *arXiv preprint arXiv:2410.15446*, 2024.
- [88] K. Chauhan *et al.*, “Interactive concept bottleneck models,” in *AAAI*, vol. 37, no. 5, 2023, pp. 5948–5955.
- [89] C. Patrício, J. C. Neves, and L. F. Teixeira, “Coherent concept-based explanations in medical image and its application to skin lesion diagnosis,” in *CVPR*, 2023, pp. 3799–3808.
- [90] S. Yan *et al.*, “Towards trustable skin cancer diagnosis via rewriting model’s decision,” in *CVPR*, 2023, pp. 11 568–11 577.
- [91] Y. Bie, L. Luo, and H. Chen, “Mica: Towards explainable skin lesion diagnosis via multi-level image-concept alignment,” in *AAAI*, vol. 38, no. 2, 2024, pp. 837–845.
- [92] R. Marcinkevičs *et al.*, “Interpretable and intervenable ultrasonography-based machine learning models for pediatric appendicitis,” *MedIA*, vol. 91, p. 103042, 2024.
- [93] A. Lucieri *et al.*, “Exaid: A multimodal explanation framework for computer-aided diagnosis of skin lesions,” *Computer Methods and Programs in Biomedicine*, vol. 215, p. 106620, 2022.
- [94] R. Jalaboi *et al.*, “Dermx: An end-to-end framework for explainable automated dermatological diagnosis,” *MedIA*, vol. 83, p. 102647, 2023.
- [95] C. Kim *et al.*, “Transparent medical image ai via an image-text foundation model grounded in medical literature,” *Nature Medicine*, pp. 1–12, 2024.
- [96] W. Pang *et al.*, “Integrating clinical knowledge into concept bottleneck models,” in *MICCAI*, 2024.
- [97] C. Wen *et al.*, “Concept-based lesion aware transformer for interpretable retinal disease diagnosis,” *TMI*, 2024.
- [98] Y. Gao *et al.*, “Aligning human knowledge with visual concepts towards explainable medical image classification,” in *MICCAI*. Springer, 2024, pp. 46–56.
- [99] Z. Chen, Y. Bei, and C. Rudin, “Concept whitening for interpretable image recognition,” *Nature Machine Intelligence*, vol. 2, no. 12, pp. 772–782, 2020.
- [100] J. Hou, J. Xu, and H. Chen, “Concept-attention whitening for interpretable skin lesion diagnosis,” in *MICCAI*. Springer, 2024, pp. 113–123.
- [101] G. Zhao *et al.*, “Diagnose like a radiologist: Hybrid neuro-probabilistic reasoning for attribute-based medical image diagnosis,” *TPAMI*, vol. 44, no. 11, pp. 7400–7416, 2021.
- [102] A. Sarkar *et al.*, “A framework for learning ante-hoc explainable models via concepts,” in *CVPR*, 2022, pp. 10 286–10 295.
- [103] Z. Fang *et al.*, “Concept-based explanation for fine-grained images and its application in infectious keratitis classification,” in *ACM MM*, 2020, pp. 700–708.
- [104] Y. Yang *et al.*, “Language in a bottle: Language model guided concept bottlenecks for interpretable image classification,” in *CVPR*, 2023, pp. 19 187–19 197.
- [105] T. Brown *et al.*, “Language models are few-shot learners,” *NeurIPS*, vol. 33, pp. 1877–1901, 2020.
- [106] A. Radford *et al.*, “Learning transferable visual models from natural language supervision,” in *ICML*. PMLR, 2021, pp. 8748–8763.
- [107] T. Oikarinen *et al.*, “Label-free concept bottleneck models,” in *ICLR*, 2023.
- [108] I. Kim *et al.*, “Concept bottleneck with visual concept filtering for explainable medical image classification,” in *MICCAI*. Springer, 2023, pp. 225–233.
- [109] J. Liu *et al.*, “A chatgpt aided explainable framework for zero-shot medical image diagnosis,” in *ICML 3rd Workshop on Interpretable Machine Learning in Healthcare (IMLH)*, 2023.

- [110] C. Patrício, L. F. Teixeira, and J. C. Neves, "Towards concept-based interpretability of skin lesion diagnosis using vision-language models," in *ISBI*. IEEE, 2024, pp. 1–5.
- [111] Y. Bie *et al.*, "Xcoop: Explainable prompt learning for computer-aided diagnosis via concept-guided context optimization," in *MICCAI*. Springer, 2024, pp. 773–783.
- [112] E. Kim *et al.*, "Xprotonet: diagnosis in chest radiography with global and local explanations," in *CVPR*, 2021, pp. 15 719–15 728.
- [113] I. Biederman, "Recognition-by-components: a theory of human image understanding." *Psychological Review*, vol. 94, no. 2, p. 115, 1987.
- [114] C. Chen *et al.*, "This looks like that: deep learning for interpretable image recognition," *NeurIPS*, vol. 32, 2019.
- [115] D. Rymarczyk *et al.*, "Protopshare: Prototypical parts sharing for similarity discovery in interpretable image classification," in *SIGKDD*, 2021, pp. 1420–1430.
- [116] D. Rymarczyk *et al.*, "Interpretable image classification with differentiable prototypes assignment," in *ECCV*. Springer, 2022, pp. 351–368.
- [117] J. Donnelly, A. J. Barnett, and C. Chen, "Deformable protopnet: An interpretable image classifier using deformable prototypes," in *CVPR*, 2022, pp. 10 265–10 275.
- [118] J. Wang *et al.*, "Interpretable image recognition by constructing transparent embedding space," in *ICCV*, 2021, pp. 895–904.
- [119] B. Wang *et al.*, "Learning bottleneck concepts in image classification," in *CVPR*, 2023, pp. 10 962–10 971.
- [120] P. Hase *et al.*, "Interpretable image recognition with hierarchical prototypes," in *Proceedings of the AAAI Conference on Human Computation and Crowdsourcing*, vol. 7, 2019, pp. 32–40.
- [121] Y. Ukai *et al.*, "This looks like it rather than that: Protoknn for similarity-based classifiers," in *ICLR*, 2022.
- [122] A. Bontempelli *et al.*, "Concept-level debugging of part-prototype networks," in *ICLR*, 2023.
- [123] G. Singh and K.-C. Yow, "An interpretable deep learning model for covid-19 detection with chest x-ray images," *IEEE Access*, vol. 9, pp. 85 198–85 208, 2021.
- [124] S. Mohammadjafari *et al.*, "Using protopnet for interpretable alzheimer's disease classification." in *Canadian Conference on AI*, 2021.
- [125] G. Carloni *et al.*, "On the applicability of prototypical part learning in medical images: breast masses classification using protopnet," in *International Conference on Pattern Recognition (ICPR)*. Springer, 2022, pp. 539–557.
- [126] C. Wang *et al.*, "Knowledge distillation to ensemble global and interpretable prototype-based mammogram classification models," in *MICCAI*. Springer, 2022, pp. 14–24.
- [127] A. J. Barnett *et al.*, "A case-based interpretable deep learning model for classification of mass lesions in digital mammography," *Nature Machine Intelligence*, vol. 3, no. 12, pp. 1061–1070, 2021.
- [128] Y. Wei, R. Tam, and X. Tang, "Mprotonet: A case-based interpretable model for brain tumor classification with 3d multi-parametric magnetic resonance imaging," in *Medical Imaging with Deep Learning*. PMLR, 2024, pp. 1798–1812.
- [129] L. S. Hesse, N. K. Dinsdale, and A. I. L. Namburete, "Prototype learning for explainable brain age prediction," in *Proceedings of the IEEE/CVF Winter Conference on Applications of Computer Vision (WACV)*, January 2024, pp. 7903–7913.
- [130] L. S. Hesse and A. I. Namburete, "Insightr-net: interpretable neural network for regression using similarity-based comparisons to prototypical examples," in *MICCAI*. Springer, 2022, pp. 502–511.
- [131] I. B. d. A. Santos and A. C. de Carvalho, "Protoal: Interpretable deep active learning with prototypes for medical imaging," *arXiv preprint arXiv:2404.04736*, 2024.
- [132] O. Li *et al.*, "Deep learning for case-based reasoning through prototypes: A neural network that explains its predictions," in *AAAI*, vol. 32, no. 1, 2018.
- [133] Q. Huang *et al.*, "Evaluation and improvement of interpretability for self-explainable part-prototype networks," in *ICCV*, 2023, pp. 2011–2020.
- [134] A. Tan, Z. Fengtao, and H. Chen, "Post-hoc part-prototype networks," in *ICML*, 2024.
- [135] M. Nauta, R. Van Bree, and C. Seifert, "Neural prototype trees for interpretable fine-grained image recognition," in *CVPR*, 2021, pp. 14 933–14 943.
- [136] M. Nauta *et al.*, "Pip-net: Patch-based intuitive prototypes for interpretable image classification," in *CVPR*, 2023, pp. 2744–2753.
- [137] C. Ma *et al.*, "This looks like those: Illuminating prototypical concepts using multiple visualizations," *NeurIPS*, vol. 36, 2024.
- [138] J. Kim, M. Kim, and Y. M. Ro, "Interpretation of lesional detection via counterfactual generation," in *2021 IEEE International Conference on Image Processing (ICIP)*. IEEE, 2021, pp. 96–100.
- [139] P. Pino *et al.*, "Clinically correct report generation from chest x-rays using templates," in *International Workshop on Machine Learning in Medical Imaging*, 2021, pp. 654–663.
- [140] I. Rodin *et al.*, "Multitask and multimodal neural network model for interpretable analysis of x-ray images," in *2019 IEEE International Conference on Bioinformatics and Biomedicine (BIBM)*. IEEE, 2019, pp. 1601–1604.
- [141] W. Gale *et al.*, "Producing radiologist-quality reports for interpretable deep learning," in *ISBI*. IEEE, 2019, pp. 1275–1279.
- [142] C. E. Lipscomb, "Medical subject headings (mesh)," *Bulletin of the Medical Library Association*, vol. 88, no. 3, p. 265, 2000.
- [143] H.-C. Shin *et al.*, "Learning to read chest x-rays: Recurrent neural cascade model for automated image annotation," in *CVPR*, 2016, pp. 2497–2506.
- [144] A. Gasimova, "Automated enriched medical concept generation for chest x-ray images," in *International Workshop on Multimodal Learning for Clinical Decision Support*, 2019, pp. 83–92.
- [145] Z. Zhang *et al.*, "Mdnet: A semantically and visually interpretable medical image diagnosis network," in *CVPR*, 2017, pp. 6428–6436.
- [146] Z. Zhang *et al.*, "Tandemnet: Distilling knowledge from medical images using diagnostic reports as optional semantic references," in *MICCAI*, 2017, pp. 320–328.
- [147] K. Ma *et al.*, "A pathology image diagnosis network with visual interpretability and structured diagnostic report," in *ICONIP*, 2018, pp. 282–293.
- [148] X. Wang *et al.*, "A computational framework towards medical image explanation," in *International Workshop on Knowledge Representation for Health Care*, 2019, pp. 120–131.
- [149] J. T. Wu *et al.*, "Chest imagenome dataset for clinical reasoning," in *NeurIPS*, 2021.
- [150] Q. Li *et al.*, "Anatomical structure-guided medical vision-language pre-training," in *MICCAI*. Springer, 2024, pp. 80–90.
- [151] T. Tanida *et al.*, "Interactive and explainable region-guided radiology report generation," in *CVPR*, 2023, pp. 7433–7442.
- [152] L. Wang *et al.*, "An inclusive task-aware framework for radiology report generation," in *MICCAI*. Springer, 2022, pp. 568–577.
- [153] S. Singh *et al.*, "From chest x-rays to radiology reports: a multimodal machine learning approach," in *2019 Digital Image Computing: Techniques and Applications (DICTA)*. IEEE, 2019, pp. 1–8.
- [154] G. Spinks and M.-F. Moens, "Justifying diagnosis decisions by deep neural networks," *Journal of Biomedical Informatics*, vol. 96, p. 103248, 2019.
- [155] G. Liu *et al.*, "Clinically accurate chest x-ray report generation," in *Machine Learning for Healthcare Conference*. PMLR, 2019, pp. 249–269.
- [156] Z. Chen *et al.*, "Generating radiology reports via memory-driven transformer," in *Proceedings of the 2020 Conference on Empirical Methods in Natural Language Processing*, 2020, pp. 1439–1449.
- [157] Z. Wang *et al.*, "Mettransformer: Radiology report generation by transformer with multiple learnable expert tokens," in *CVPR*, 2023, pp. 11 558–11 567.
- [158] J. Yuan *et al.*, "Automatic radiology report generation based on multi-view image fusion and medical concept enrichment," in *MICCAI*, 2019, pp. 721–729.
- [159] H. Lee, S. Kim, and Y. Ro, "Generation of multimodal justification using visual word constraint model for explainable computer-aided diagnosis," in *Interpretability of Machine Intelligence in Medical Computing and Multimodal Learning for Clinical Decision Support*. Springer, 2019.
- [160] Z. Zhang *et al.*, "Pathologist-level interpretable whole-slide cancer diagnosis with deep learning," *Nature Machine Intelligence*, vol. 1, no. 5, pp. 236–245, 2019.
- [161] X. Wang *et al.*, "Tienet: Text-image embedding network for common thorax disease classification and reporting in chest x-rays," in *CVPR*, 2018, pp. 9049–9058.
- [162] B. Jing, P. Xie, and E. Xing, "On the automatic generation of medical imaging reports," in *Proceedings of the 56th Annual Meeting of the Association for Computational Linguistics (ACL)*, 2018, pp. 2577–2586.
- [163] X. Zeng *et al.*, "Generating diagnostic report for medical image by high-middle-level visual information incorporation on double deep learning models," *Computer Methods and Programs in Biomedicine*, vol. 197, p. 105700, 2020.

- [164] J. Tian *et al.*, “A diagnostic report generator from ct volumes on liver tumor with semi-supervised attention mechanism,” in *MICCAI*, 2018, pp. 702–710.
- [165] O. Thawkar *et al.*, “Xraygpt: Chest radiographs summarization using medical vision-language models,” *arXiv preprint arXiv:2306.07971*, 2023.
- [166] J. Zhou *et al.*, “Pre-trained multimodal large language model enhances dermatological diagnosis using skin-gpt-4,” *Nature Communications*, vol. 15, no. 1, p. 5649, 2024.
- [167] M. Moor *et al.*, “Med-flamingo: a multimodal medical few-shot learner,” in *Machine Learning for Health (MLAH)*. PMLR, 2023, pp. 353–367.
- [168] C. Li *et al.*, “Llava-med: Training a large language-and-vision assistant for biomedicine in one day,” *NeurIPS*, vol. 36, 2024.
- [169] S. He *et al.*, “Meddr: Diagnosis-guided bootstrapping for large-scale medical vision-language learning,” *arXiv preprint arXiv:2404.15127*, 2024.
- [170] J. Chen *et al.*, “Huatogpt-vision, towards injecting medical visual knowledge into multimodal llms at scale,” *arXiv preprint arXiv:2406.19280*, 2024.
- [171] S. Kang *et al.*, “Wolf: Large language model framework for cxr understanding,” *arXiv preprint arXiv:2403.15456*, 2024.
- [172] Z. Chen *et al.*, “Chexagent: Towards a foundation model for chest x-ray interpretation,” *arXiv preprint arXiv:2401.12208*, 2024.
- [173] K. Schutte *et al.*, “Using stylegan for visual interpretability of deep learning models on medical images,” *arXiv preprint arXiv:2101.07563*, 2021.
- [174] I. Goodfellow *et al.*, “Generative adversarial nets,” *NeurIPS*, vol. 27, 2014.
- [175] T. Laugel *et al.*, “Issues with post-hoc counterfactual explanations: a discussion,” in *ICML Workshop on Human in the Loop Learning*, 2019.
- [176] H. Guo, T. H. Nguyen, and A. Yadav, “CounterNet: End-to-end training of prediction aware counterfactual explanations,” in *SIGKDD*, 2023, pp. 577–589.
- [177] V. Guyomard *et al.*, “Vnet: A self-explaining model for realistic counterfactual generation,” in *Joint European Conference on Machine Learning and Knowledge Discovery in Databases*. Springer, 2022, pp. 437–453.
- [178] M. Wilms *et al.*, “Towards self-explainable classifiers and regressors in neuroimaging with normalizing flows,” in *International Workshop on Machine Learning in Clinical Neuroimaging*, 2021, pp. 23–33.
- [179] U. Johansson, R. König, and L. Niklasson, “The truth is in there: rule extraction from opaque models using genetic programming,” in *FLAIRS*, 2004, pp. 658–663.
- [180] H. Lakkaraju *et al.*, “Faithful and customizable explanations of black box models,” in *Proceedings of the 2019 AAAI/ACM Conference on AI, Ethics, and Society*, 2019, pp. 131–138.
- [181] W. Jin *et al.*, “Guidelines and evaluation of clinical explainable ai in medical image analysis,” *MedIA*, vol. 84, p. 102684, 2023.
- [182] M. Robnik-Šikonja and M. Bohanec, “Perturbation-based explanations of prediction models,” *Human and Machine Learning: Visible, Explainable, Trustworthy and Transparent*, pp. 159–175, 2018.
- [183] E. Lughofer *et al.*, “Explaining classifier decisions linguistically for stimulating and improving operators labeling behavior,” *Information Sciences*, vol. 420, pp. 16–36, 2017.
- [184] A. Adadi and M. Berrada, “Explainable ai for healthcare: from black box to interpretable models,” in *Embedded Systems and Artificial Intelligence*. Springer, 2020, pp. 327–337.
- [185] X. Wu *et al.*, “Usable xai: 10 strategies towards exploiting explainability in the llm era,” *arXiv preprint arXiv:2403.08946*, 2024.
- [186] F. Doshi-Velez and B. Kim, “Towards a rigorous science of interpretable machine learning,” *arXiv preprint arXiv:1702.08608*, 2017.
- [187] J. Zhou *et al.*, “Evaluating the quality of machine learning explanations: A survey on methods and metrics,” *Electronics*, vol. 10, no. 5, p. 593, 2021.
- [188] A. Holzinger, A. Carrington, and H. Müller, “Measuring the quality of explanations: the system causability scale (scs) comparing human and machine explanations,” *KI-Künstliche Intelligenz*, vol. 34, no. 2, pp. 193–198, 2020.
- [189] R. Sayres *et al.*, “Using a deep learning algorithm and integrated gradients explanation to assist grading for diabetic retinopathy,” *Ophthalmology*, vol. 126, no. 4, pp. 552–564, 2019.
- [190] V. Petsiuk, A. Das, and K. Saenko, “Rise: Randomized input sampling for explanation of black-box models,” *British Machine Vision Conference*, 2018.
- [191] S. Hooker *et al.*, “A benchmark for interpretability methods in deep neural networks,” *NeurIPS*, vol. 32, 2019.
- [192] J. Hou *et al.*, “Diabetic retinopathy grading with weakly-supervised lesion priors,” in *2023 IEEE International Conference on Acoustics, Speech and Signal Processing*. IEEE, 2023, pp. 1–5.
- [193] S. M. Muddamsetty, M. N. Jahromi, and T. B. Moeslund, “Expert level evaluations for explainable ai (xai) methods in the medical domain,” in *ICPR*. Springer, 2021, pp. 35–46.
- [194] A. J. Barnett *et al.*, “Interpretable mammographic image classification using case-based reasoning and deep learning,” *arXiv preprint arXiv:2107.05605*, 2021.
- [195] C.-K. Yeh *et al.*, “On completeness-aware concept-based explanations in deep neural networks,” *NeurIPS*, vol. 33, pp. 20 554–20 565, 2020.
- [196] A.-p. Nguyen and M. R. Martínez, “On quantitative aspects of model interpretability,” *arXiv preprint arXiv:2007.07584*, 2020.
- [197] K. Papineni *et al.*, “Bleu: a method for automatic evaluation of machine translation,” in *ACL*, 2002, pp. 311–318.
- [198] C.-Y. Lin, “Rouge: A package for automatic evaluation of summaries,” in *Text Summarization Branches Out*, 2004, pp. 74–81.
- [199] R. Vedantam, C. Lawrence Zitnick, and D. Parikh, “Cider: Consensus-based image description evaluation,” in *CVPR*, 2015, pp. 4566–4575.
- [200] R. K. Mothilal, A. Sharma, and C. Tan, “Explaining machine learning classifiers through diverse counterfactual explanations,” in *FACCT*, 2020, pp. 607–617.
- [201] S. Singla *et al.*, “Explaining the black-box smoothly—a counterfactual approach,” *MedIA*, vol. 84, p. 102721, 2023.
- [202] S. Tonekaboni *et al.*, “What clinicians want: contextualizing explainable machine learning for clinical end use,” in *Machine Learning for Healthcare Conference*. PMLR, 2019, pp. 359–380.
- [203] K. Singhal *et al.*, “Towards expert-level medical question answering with large language models,” *arXiv preprint arXiv:2305.09617*, 2023.
- [204] C. Wu *et al.*, “Pmc-llama: toward building open-source language models for medicine,” *Journal of the American Medical Informatics Association*, p. ocae045, 2024.
- [205] Y. Gu *et al.*, “Domain-specific language model pretraining for biomedical natural language processing,” *ACM Transactions on Computing for Healthcare (HEALTH)*, vol. 3, no. 1, pp. 1–23, 2021.
- [206] M. Moor *et al.*, “Foundation models for generalist medical artificial intelligence,” *Nature*, vol. 616, no. 7956, pp. 259–265, 2023.
- [207] X. Ye and G. Durrett, “Can explanations be useful for calibrating black box models?” in *ACL*, 2022, pp. 6199–6212.
- [208] X. Wu *et al.*, “From language modeling to instruction following: Understanding the behavior shift in llms after instruction tuning,” in *Proceedings of the 2024 Conference of the North American Chapter of the Association for Computational Linguistics: Human Language Technologies*, 2024, pp. 2341–2369.
- [209] J. Wei *et al.*, “Chain-of-thought prompting elicits reasoning in large language models,” *NeurIPS*, vol. 35, pp. 24 824–24 837, 2022.
- [210] Y. Shi *et al.*, “Mededit: Model editing for medical question answering with external knowledge bases,” *arXiv preprint arXiv:2309.16035*, 2023.
- [211] K. Singhal *et al.*, “Large language models encode clinical knowledge,” *Nature*, vol. 620, no. 7972, pp. 172–180, 2023.
- [212] C. Zhao *et al.*, “Automated natural language explanation of deep visual neurons with large models,” *arXiv preprint arXiv:2310.10708*, 2023.
- [213] C. Singh *et al.*, “Augmenting interpretable models with large language models during training,” *Nature Communications*, vol. 14, no. 1, p. 7913, 2023.
- [214] S. Bills *et al.*, “Language models can explain neurons in language models,” *URL https://openaiublic.blob.core.windows.net/neuron-explainer/paper/index.html.(Date accessed: 14.05. 2023)*, vol. 2, 2023.
- [215] D. Gunning and D. Aha, “Darpa’s explainable artificial intelligence (xai) program,” *AI Magazine*, vol. 40, no. 2, pp. 44–58, 2019.
- [216] D. Minh *et al.*, “Explainable artificial intelligence: a comprehensive review,” *Artificial Intelligence Review*, pp. 1–66, 2022.
- [217] C. Rudin *et al.*, “Interpretable machine learning: Fundamental principles and 10 grand challenges,” *Statistic Surveys*, vol. 16, pp. 1–85, 2022.
- [218] Y. Xu and H. Chen, “Multimodal optimal transport-based co-attention transformer with global structure consistency for survival prediction,” in *ICCV*, 2023, pp. 21 241–21 251.
- [219] J. Pearl, *Causality*. Cambridge university press, 2009.
- [220] A. J. DeGrave, J. D. Janizek, and S.-I. Lee, “Ai for radiographic covid-19 detection selects shortcuts over signal,” *Nature Machine Intelligence*, vol. 3, no. 7, pp. 610–619, 2021.
- [221] D. C. Castro, I. Walker, and B. Glocker, “Causality matters in medical imaging,” *Nature Communications*, vol. 11, no. 1, p. 3673, 2020.
- [222] L. Luo *et al.*, “Pseudo bias-balanced learning for debiased chest x-ray classification,” in *MICCAI*. Springer, 2022, pp. 621–631.

- [223] X. He *et al.*, "Pathvqa: 30000+ questions for medical visual question answering," *arXiv preprint arXiv:2003.10286*, 2020.
- [224] X. Wang *et al.*, "Chestx-ray8: Hospital-scale chest x-ray database and benchmarks on weakly-supervised classification and localization of common thorax diseases," in *CVPR*, 2017, pp. 2097–2106.
- [225] D. Demner-Fushman *et al.*, "Preparing a collection of radiology examinations for distribution and retrieval," *Journal of the American Medical Informatics Association*, vol. 23, no. 2, pp. 304–310, 2016.
- [226] A. E. Johnson *et al.*, "Mimic-cxr, a de-identified publicly available database of chest radiographs with free-text reports," *Scientific data*, vol. 6, no. 1, p. 317, 2019.
- [227] J. Irvin *et al.*, "Chexpert: A large chest radiograph dataset with uncertainty labels and expert comparison," in *AAAI*, vol. 33, no. 01, 2019, pp. 590–597.
- [228] N. C. Institute, "The cancer genome atlas program," 2006. [Online]. Available: <https://www.cancer.gov/tcga>
- [229] M. Heath *et al.*, "Current status of the digital database for screening mammography," in *Digital Mammography: Nijmegen, 1998*. Springer, 1998, pp. 457–460.
- [230] A. Diaz-Pinto *et al.*, "Cnns for automatic glaucoma assessment using fundus images: an extensive validation," *Biomedical engineering online*, vol. 18, pp. 1–19, 2019.
- [231] J. Arevalo *et al.*, "Representation learning for mammography mass lesion classification with convolutional neural networks," *Computer methods and programs in biomedicine*, vol. 127, pp. 248–257, 2016.
- [232] H. R. Roth *et al.*, "Hierarchical 3d fully convolutional networks for multi-organ segmentation," *arXiv preprint arXiv:1704.06382*, 2017.
- [233] H. R. Roth *et al.*, "Data from pancreas-ct. the cancer imaging archive," *IEEE Transactions on Image Processing*, vol. 10, p. K9, 2016.
- [234] B. T. Wyman *et al.*, "Standardization of analysis sets for reporting results from adni mri data," *Alzheimer's & Dementia*, vol. 9, no. 3, pp. 332–337, 2013.
- [235] C. R. Jack Jr *et al.*, "Update on the magnetic resonance imaging core of the alzheimer's disease neuroimaging initiative," *Alzheimer's & Dementia*, vol. 6, no. 3, pp. 212–220, 2010.
- [236] N. Codella *et al.*, "Skin lesion analysis toward melanoma detection 2018: A challenge hosted by the international skin imaging collaboration (isic)," *arXiv preprint arXiv:1902.03368*, 2019.
- [237] R. Souza *et al.*, "An open, multi-vendor, multi-field-strength brain mr dataset and analysis of publicly available skull stripping methods agreement," *NeuroImage*, vol. 170, pp. 482–494, 2018.
- [238] G. Shih *et al.*, "Augmenting the national institutes of health chest radiograph dataset with expert annotations of possible pneumonia," *Radiology: Artificial Intelligence*, vol. 1, no. 1, p. e180041, 2019.
- [239] D. S. Kermany *et al.*, "Identifying medical diagnoses and treatable diseases by image-based deep learning," *Cell*, vol. 172, no. 5, pp. 1122–1131, 2018.
- [240] P. Lakhani *et al.*, "The 2021 siim-fisabio-rsna machine learning covid-19 challenge: Annotation and standard exam classification of covid-19 chest radiographs," *Journal of Digital Imaging*, vol. 36, no. 1, pp. 365–372, 2023.
- [241] M. E. Chowdhury *et al.*, "Can ai help in screening viral and covid-19 pneumonia?" *IEEE Access*, vol. 8, pp. 132 665–132 676, 2020.
- [242] T. Rahman *et al.*, "Exploring the effect of image enhancement techniques on covid-19 detection using chest x-ray images," *Computers in biology and medicine*, vol. 132, p. 104319, 2021.
- [243] J. Saltz *et al.*, "Stony brook university covid-19 positive cases," *The Cancer Imaging Archive*, vol. 4, 2021.
- [244] E. Tsai *et al.*, "Data from medical imaging data resource center (midrc)-rsna international covid radiology database (ricord) release 1c-chest x-ray, covid+(midrc-ricord-1c)," *The Cancer Imaging Archive*, vol. 10, 2021.
- [245] E. B. Tsai *et al.*, "The rsna international covid-19 open radiology database (ricord)," *Radiology*, vol. 299, no. 1, pp. E204–E213, 2021.
- [246] X. Wang *et al.*, "Hospital-scale chest x-ray database and benchmarks on weakly-supervised classification and localization of common thorax diseases," in *IEEE CVPR*, vol. 7. sn, 2017, p. 46.
- [247] H. Q. Nguyen *et al.*, "Vindr-cxr: An open dataset of chest x-rays with radiologist's annotations," *Scientific Data*, vol. 9, no. 1, p. 429, 2022.
- [248] G. Aresta *et al.*, "Bach: Grand challenge on breast cancer histology images," *MedIA*, vol. 56, pp. 122–139, 2019.
- [249] D. Gutman *et al.*, "Skin lesion analysis toward melanoma detection: A challenge at the international symposium on biomedical imaging (isbi) 2016, hosted by the international skin imaging collaboration (isic)," *arXiv preprint arXiv:1605.01397*, 2016.
- [250] N. C. Codella *et al.*, "Skin lesion analysis toward melanoma detection: A challenge at the 2017 international symposium on biomedical imaging (isbi), hosted by the international skin imaging collaboration (isic)," in *ISBI*. IEEE, 2018, pp. 168–172.
- [251] F. Heinemann, G. Birk, and B. Stierstorfer, "Deep learning enables pathologist-like scoring of nash models," *Scientific reports*, vol. 9, no. 1, p. 18454, 2019.
- [252] P. Radau *et al.*, "Evaluation framework for algorithms segmenting short axis cardiac mri," *The MIDAS Journal*, 2009.
- [253] O. Bernard *et al.*, "Deep learning techniques for automatic mri cardiac multi-structures segmentation and diagnosis: is the problem solved?" *TMI*, vol. 37, no. 11, pp. 2514–2525, 2018.
- [254] P. Tschandl, C. Rosendahl, and H. Kittler, "The ham10000 dataset, a large collection of multi-source dermatoscopic images of common pigmented skin lesions. scientific data. 2018; 5: 180161," *Search in*, vol. 2, 2018.
- [255] C. for Biomedical Image Computing and Analytics, "Multimodal brain tumor segmentation challenge 2020: Data," *MICCAI 2020 BraTs*, 2020. [Online]. Available: <https://www.med.upenn.edu/cbica/brats2020/data.html>
- [256] A. E. Kavrur *et al.*, "Chaos challenge-combined (ct-mr) healthy abdominal organ segmentation," *MedIA*, vol. 69, p. 101950, 2021.
- [257] M. Combalia *et al.*, "Bcn20000: Dermoscopic lesions in the wild," *arXiv preprint arXiv:1908.02288*, 2019.
- [258] M. Nevitt, D. Felson, and G. Lester, "The osteoarthritis initiative," *Protocol for the cohort study*, vol. 1, p. 2, 2006.
- [259] J. Kawahara *et al.*, "Seven-point checklist and skin lesion classification using multitask multimodal neural nets," *JBHI*, vol. 23, no. 2, pp. 538–546, 2018.
- [260] T. Mendonça *et al.*, "Ph2: A public database for the analysis of dermoscopic images," *Dermoscopy image analysis*, vol. 2, 2015.
- [261] R. Daneshjou *et al.*, "Skincon: A skin disease dataset densely annotated by domain experts for fine-grained debugging and analysis," *NeurIPS*, vol. 35, pp. 18 157–18 167, 2022.
- [262] N. Z. D. Society, "Dermatology images." [Online]. Available: <https://dermnetnz.org/>
- [263] X. Sun *et al.*, "A benchmark for automatic visual classification of clinical skin disease images," in *Computer Vision—ECCV 2016: 14th European Conference, Amsterdam, The Netherlands, October 11–14, 2016, Proceedings, Part VI 14*. Springer, 2016, pp. 206–222.
- [264] M. Groh *et al.*, "Evaluating deep neural networks trained on clinical images in dermatology with the fitzpatrick 17k dataset," in *CVPR*, 2021, pp. 1820–1828.
- [265] R. Daneshjou *et al.*, "Disparities in dermatology ai performance on a diverse, curated clinical image set," *Science advances*, vol. 8, no. 31, p. eabq6147, 2022.
- [266] S. Tsutsui, W. Pang, and B. Wen, "Wbcatt: a white blood cell dataset annotated with detailed morphological attributes," *NeurIPS*, vol. 36, 2024.
- [267] Y. Zhou *et al.*, "A benchmark for studying diabetic retinopathy: segmentation, grading, and transferability," *TMI*, vol. 40, no. 3, pp. 818–828, 2020.
- [268] T. Li *et al.*, "Diagnostic assessment of deep learning algorithms for diabetic retinopathy screening," *Information Sciences*, vol. 501, pp. 511–522, 2019.
- [269] J. N. Kather, N. Halama, and A. Marx, "100,000 histological images of human colorectal cancer and healthy tissue," *Zenodo10*, vol. 5281, no. 9, 2018.
- [270] P. Porwal *et al.*, "Indian diabetic retinopathy image dataset (idrid): a database for diabetic retinopathy screening research," *Data*, vol. 3, no. 3, p. 25, 2018.
- [271] W. Al-Dhabyani *et al.*, "Deep learning approaches for data augmentation and classification of breast masses using ultrasound images," *Int. J. Adv. Comput. Sci. Appl*, vol. 10, no. 5, pp. 1–11, 2019.
- [272] S. G. Armato III *et al.*, "The lung image database consortium (lide) and image database resource initiative (idri): a completed reference database of lung nodules on ct scans," *Medical physics*, vol. 38, no. 2, pp. 915–931, 2011.
- [273] Y. Xu *et al.*, "Deep sequential feature learning in clinical image classification of infectious keratitis," *Engineering*, vol. 7, no. 7, pp. 1002–1010, 2021.
- [274] S. Jaeger *et al.*, "Two public chest x-ray datasets for computer-aided screening of pulmonary diseases," *Quantitative imaging in medicine and surgery*, vol. 4, no. 6, p. 475, 2014.
- [275] D. Demner-Fushman *et al.*, "Design and development of a multimodal biomedical information retrieval system," *Journal of Computing Science and Engineering*, vol. 6, no. 2, pp. 168–177, 2012.

- [276] J. P. Cohen, P. Morrison, and L. Dao, "Covid-19 image data collection," *arXiv preprint arXiv:2003.11597*, 2020.
- [277] D. S. Marcus *et al.*, "Open access series of imaging studies (oasis): cross-sectional mri data in young, middle aged, nondemented, and demented older adults," *Journal of Cognitive Neuroscience*, vol. 19, no. 9, pp. 1498–1507, 2007.
- [278] R. S. Lee *et al.*, "A curated mammography data set for use in computer-aided detection and diagnosis research," *Scientific data*, vol. 4, no. 1, pp. 1–9, 2017.
- [279] C. Cui *et al.*, "The chinese mammography database (cmmd): An online mammography database with biopsy confirmed types for machine diagnosis of breast," *The Cancer Imaging Archive*, vol. 1, 2021.
- [280] B. H. Menze *et al.*, "The multimodal brain tumor image segmentation benchmark (brats)," *TMI*, vol. 34, no. 10, pp. 1993–2024, 2014.
- [281] <https://brain-development.org/ixi-dataset/>.
- [282] A. T. Papageorghiou *et al.*, "International standards for fetal growth based on serial ultrasound measurements: the fetal growth longitudinal study of the intergrowth-21st project," *The Lancet*, vol. 384, no. 9946, pp. 869–879, 2014.
- [283] C. H. Foundation, "Eyepacs," 2015. [Online]. Available: <https://www.kaggle.com/c/diabetic-retinopathy-detection/data>
- [284] E. Decencière *et al.*, "Feedback on a publicly distributed image database: The messidor database. image anal & stereology 33: 231–234," 2014.
- [285] Y. Kim *et al.*, "Adversarially regularized autoencoders for generating discrete structures," *arXiv preprint arXiv:1706.04223*, vol. 2, p. 12, 2017.
- [286] K. N. Jones *et al.*, "Peir digital library: Online resources and authoring system," in *Proceedings of the AMIA Symposium*. American Medical Informatics Association, 2001, p. 1075.
- [287] P. Bilic *et al.*, "The liver tumor segmentation benchmark (lits)," *MedIA*, vol. 84, p. 102680, 2023.
- [288] kaggle, "Dermnet," [Online]. Available: <https://www.kaggle.com/datasets/shubhamgoel27/dermnet>
- [289] W. Lin *et al.*, "Pmc-clip: Contrastive language-image pre-training using biomedical documents," in *MICCAI*. Springer, 2023, pp. 525–536.
- [290] J. J. Lau *et al.*, "A dataset of clinically generated visual questions and answers about radiology images," *Scientific data*, vol. 5, no. 1, pp. 1–10, 2018.
- [291] X. Zhang *et al.*, "Pmc-vqa: Visual instruction tuning for medical visual question answering," *arXiv preprint arXiv:2305.10415*, 2023.
- [292] S. Bae *et al.*, "Ehrxqa: A multi-modal question answering dataset for electronic health records with chest x-ray images," *NeurIPS*, vol. 36, 2024.
- [293] J. Wu *et al.*, "Chest imagenome dataset," *Physio Net*, 2021.
- [294] H. Cai *et al.*, "Breast microcalcification diagnosis using deep convolutional neural network from digital mammograms," *Computational and mathematical methods in medicine*, vol. 2019, no. 1, p. 2717454, 2019.
- [295] G. Argenziano *et al.*, "Epiluminescence microscopy for the diagnosis of doubtful melanocytic skin lesions: comparison of the abcd rule of dermatoscopy and a new 7-point checklist based on pattern analysis," *Archives of dermatology*, vol. 134, no. 12, pp. 1563–1570, 1998.
- [296] H. Borgli *et al.*, "Hyperkvasir, a comprehensive multi-class image and video dataset for gastrointestinal endoscopy," *Scientific data*, vol. 7, no. 1, p. 283, 2020.